

Digital Elevation Model Offshore Taiwan and Its Tectonic Implications

Char-Shine Liu¹, Shao-Yung Liu², Serge E. Lallemand³, Neil Lundberg⁴ and Donald L. Reed⁵

(Manuscript received 17 August 1998, in final form 16 November 1998)

ABSTRACT

A new 500-m gridded digital bathymetric data set has been produced by compiling available shipboard bathymetric data supplemented by global bathymetric data sets in the area between 18°N and 27°N, and from 117°E to 125°E. Combined with topographic data from GTOPO30, a global land data set in 30 arc-second grid spacing, this new digital elevation model (DEM) reveals the regional as well as local morphology of Taiwan and its offshore area. Spatial resolution of 1 km is achieved in the area off eastern and southern Taiwan where swath bathymetric data are available. In other areas where ship tracks are sparse, a spatial resolution of 4 arc-minute is retained. This DEM provides the best topographic information at present on a regional scale, which helps to reveal many of the morphotectonic features related to the active tectonic processes of subduction and arc-continent collision in this region.

Using 2-D shaded topographic maps and 3-D physiographic diagrams generated from the DEM, the major morphologic features in each tectonic province of the region are presented. The Taiwan Strait is characterized by low relief sea floor with two NE-SW trending depressions and a shallow bank in the center of the strait. Submarine canyons mark the continental slope. In the area off southern Taiwan, N-S trending ridges and troughs are the major morphological features, however, several NE-SW trending lineaments have been identified in the Luzon forearc region. Off eastern Taiwan, submarine canyons and topographic features related to sedimentary processes along the eastern flank of the Luzon Arc are revealed in detail. A prominent N-S trending linear ridge, the Gagua Ridge, located along 123°E on the West Philippine Basin floor is entering the Ryukyu Trench and has produced a big re-entrant at the frontal portion of the Yaeyama Ridge. E-

¹Institute of Oceanography, National Taiwan University, Taipei, Taiwan, ROC

²Institute of Oceanography, National Taiwan University, Taipei, Taiwan, ROC

Presently at: National Center for Ocean Research, P.O. Box 23-13, Taipei, Taiwan, ROC

³UMR 5573, Laboratoire de Geophysique et Tectonique, Universite de Montpellier 2, France

⁴Department of Geology, Florida State University, Tallahassee, FL 32306, USA

⁵Department of Geology, San Jose State University, San Jose, CA 95192, USA

W to NW-SE trending linear shear zones are observed over the Yaeyama Ridge. These linear faults are the results of westward migration of the frontal portion of the accretionary wedge due to oblique convergence. A series of four forearc basins have been identified. Different depths of the forearc basins reflect lateral variation of the forearc region from oblique subduction to collision. Along the northern wall of the Southern Okinawa Trough, faulted slope and subsided shelf blocks suggest that this region is under post-collisional extension, and the active extension of the Southern Okinawa Trough is advancing westward toward Taiwan.

(Key words: Digital Elevation Model, Swath bathymetry, Seafloor Morphology, Morphotectonic structures, Taiwan offshore region)

1. INTRODUCTION

Geomorphology is the study of the shape of the Earth's surface. Bathymetric measurements provide morphologic information of the seafloor. The shape of the seafloor is often controlled by tectonic processes and modified by submarine erosional and depositional processes. In many parts of the ocean, bathymetry is the only type of geological information available. Thus, compared to land, seafloor topography plays a larger role in geologic interpretations (Vogt and Tucholke, 1986). This is especially true in a tectonically active region where morphotectonic characteristics of the seafloor provide critical constraints on the structures and tectonic processes, which produce the submarine topography.

Taiwan and its adjacent offshore area is a tectonically active region. Located at the western tip of the Philippine Sea plate, the Taiwan mountain belt was formed by the collision of the Luzon volcanic arc with the passive continental margin of the Eurasia plate in the last 5 Ma (Ho, 1986; Teng, 1990). South of Taiwan, oceanic lithosphere of the South China Sea (Eurasia plate) is subducting eastward underneath the Philippine Sea plate along the Manila Trench-Luzon Arc system; whereas east of Taiwan, the Philippine Sea plate is subducting northwestward beneath the Eurasia plate along the Ryukyu arc-trench system. Complicated morphotectonic features associated with plate subduction (such as trench, accretionary wedge, forearc basin, arc, and backarc basin) and arc-continent collision (such as faulting, folding, block rotation, plate deformation, etc.) are all presented off eastern and off southern Taiwan (Figure 1). On the other hand, west of Taiwan, small topographic relief indicates that structures of the Tertiary sedimentary basins along the passive Chinese continental margin are still preserved (Sun, 1982; Yu, 1993).

It has long been known that the seafloor west of Taiwan is shallow and flat (Yabe and Tayama, 1928) while the water depth increases rapidly off east coast of Taiwan (Figure 1). Though Ma (1947) mentioned that the soundings available in the published marine charts were not adequate to draw desired contour lines for water depth beyond 2,000 meters, the submarine topographic map he published in the nearshore areas around the southern part of Taiwan (Figure 1 of Ma, 1947) is quite good even viewed from today. Early observation of the seafloor topography around Taiwan were largely based on the charts from the Chinese Navy

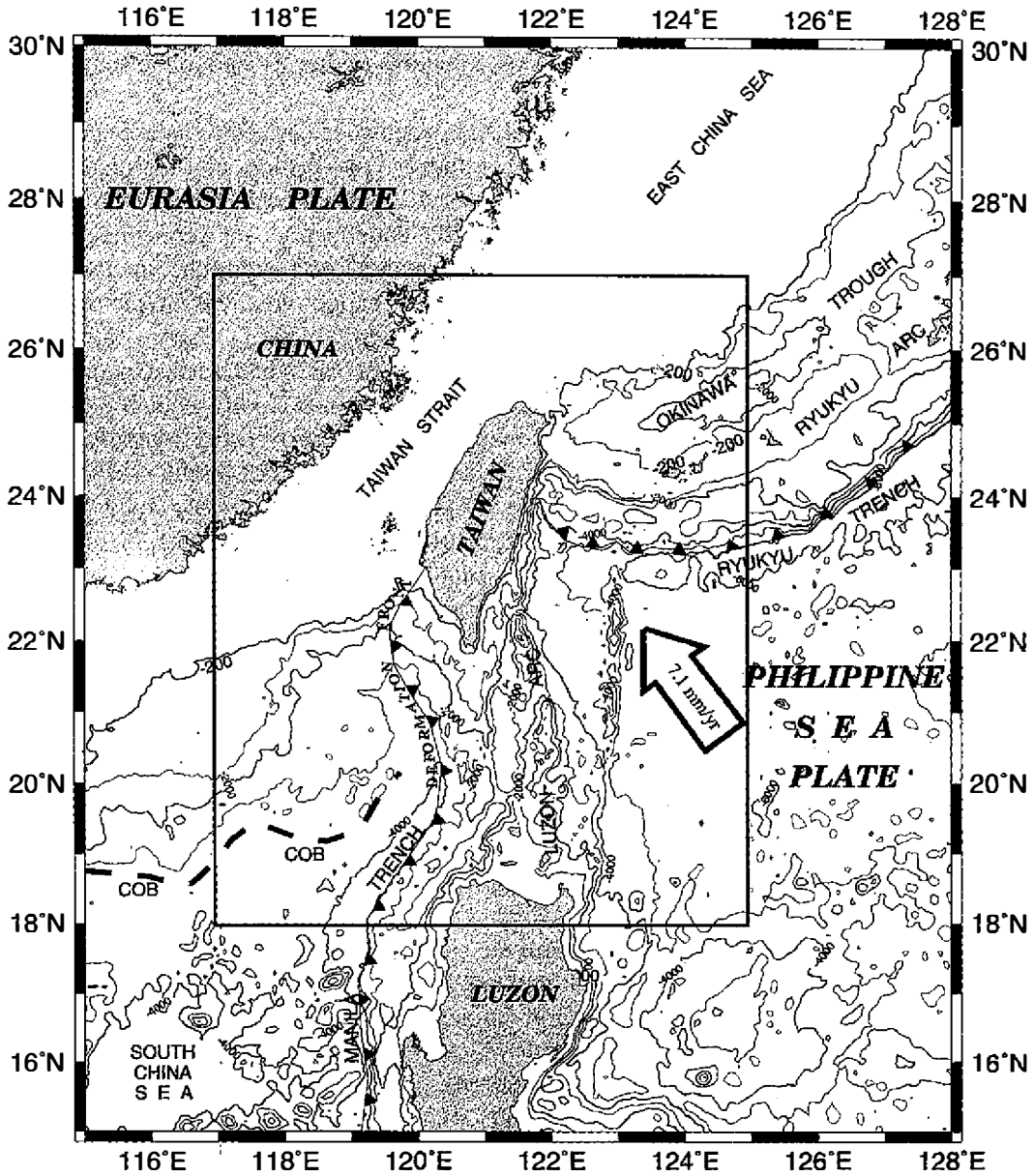


Fig. 1. Tectonic setting of the Eurasia plate and Philippine Sea plate near Taiwan. The arrow indicates the relative convergent direction and the number inside the arrow shows the amount of convergence based on Seno *et al.* (1993). Lines with teeth show the location of subduction zones. Dashed line annotated with COB marks the continent ocean boundary of Taylor and Hayes (1983). Box shows the area covered by the new DEM.

and from the U.S. Naval Oceanographic Office (*e.g.*, Chase and Menard, 1969). It was not until Mammerickx *et al.* (1976) published the bathymetry chart of the East and Southeast Asian Seas, that major submarine morphotectonic features to the east and to the south of Taiwan were accurately revealed.

In the past two decades, marine geological and geophysical surveys conducted near Taiwan provide new bathymetric measurements that improve the resolution of regional seafloor topography (*e.g.*, Lee *et al.*, 1980; Lewis and Hayes, 1984; Chen and Juang, 1986; Sibuet *et al.*, 1987; Hsu *et al.*, 1996). However, since most of the bathymetric data were collected using single-beam depth sounders and the Transit Satellite navigation system, the hand-drawn regional bathymetric maps are of limited usage. Possible exceptions are the Bathymetric Map of the Okinawa Trough (Marsset *et al.*, 1987) and the Bathymetric Map of Offshore Taiwan (Hsu *et al.*, 1995) as both map compilations included segments of swath bathymetric data.

Starting in the late eighties, when the GPS navigation became readily available, the accuracy of ship positioning during bathymetric measurements improved substantially. Marine geological and geophysical surveys, including several international cooperative surveys, have been actively carried out in the past ten years by the Institute of Oceanography, National Taiwan University. With more high quality bathymetric data available, compilation of a bathymetric digital elevation model (hereafter DEM) using computer gridding and contouring techniques (*e.g.*, Smith and Wessel, 1990; Jones and Hamilton, 1992) became possible.

The advantages of producing a DEM rather than hand-drawn bathymetric chart are numerous. For one, bathymetric maps of various scales, contour intervals, and projections can be easily generated from the DEM. Three-dimensional topographic relief diagrams and two-dimensional hill-shading views of the DEM from selected viewing angles and azimuths often reveal specific morphological features or topographic lineaments. Maps showing slope gradients and submarine drainage patterns can also be generated. Best of all, the DEM can be easily improved with the addition of new bathymetric data.

The first digital bathymetric data set available that covers the offshore area around Taiwan is the ETOPO5 bathymetry/topography data (National Geophysical Data Center, 1988). However, this global data set provides bathymetric values averaged over a 5 minute by 5 minute grid spacing (or about 9 km by 9 km in low latitude areas), and so resolution of topographic features is inadequate for local morphological studies. Liu *et al.* (1992) produced the first local DEM for the area off southern Taiwan. Another local DEM covering the area off northeastern Taiwan was generated by Song (1994). A complete regional DEM for the offshore areas around Taiwan was released by Liu *et al.* (1996a). With a 1 arc-minute grid spacing, this first version of the Taiwan DEM reveals many detailed submarine topographic features (*e.g.*, Fuh *et al.*, 1997; Lallemand *et al.*, 1997a; Liu *et al.*, 1997a; Schnurle *et al.*, 1998a), and has been used widely as a framework of submarine topography. However, since this DEM was compiled based only on single-beam bathymetric data, both accuracy and resolution of the bathymetry can be improved.

In May and June 1996, the French research vessel L'Atalante conducted a joint Sino-French cruise (the ACT cruise) to map the seafloor east and southwest of Taiwan. High quality swath bathymetric data were collected that reveal details of the seafloor morphotectonic features (Lallemand *et al.*, 1997b). Then in late 1996, bathymetric data collected by both R/V

Ocean Researcher II and R/V Ocean Researcher III were made available to us. With the influx of new high-quality bathymetric data, we are able to generate a new DEM of the Taiwan offshore region, which covers a larger area (from 117°E to 125°E and from 18°N to 27°N) and provides much better resolution than the one released in 1996 (Liu *et al.*, 1996a).

This new DEM reveals many topographic features that were not known or not clearly imaged before. The main purpose of this paper, thus, is to provide a morphological framework of the region surrounding Taiwan. We present compilation procedures of this DEM, discuss the bathymetric resolutions for different areas with various degrees of data coverage, and describe some important topographic features around Taiwan. Since most of the topographic features are controlled by the regional active tectonic processes, we discuss their tectonic implications as well.

2. DATA COMPILATION AND USAGE

2.1. Data Sources

We have examined all the bathymetric data available for the compilation of this DEM. Four types of data are used. They are the swath bathymetric data, the underway depth sounding data from single-beam echo sounders, the digitized bathymetric data from published bathymetric maps, and the digital topographic data of the world from ETOPO5 (National Geophysical Data Center, 1988), GTOPO30 (U.S. Geological Survey, 1993), and the Measured and Estimated Seafloor Topography (MEST) of Smith and Sandwell (1997). Table 1 lists major bathymetric data sources used in this compilation. Distribution of the actual bathymetric data coverage is shown in Figure 2.

Swath bathymetric data provide the best quality and highest resolution sea floor depth information. In this study, swath bathymetric data collected during the ACT cruise of the French R/V *L'Atalante* in June 1996 (Lallemand *et al.*, 1997b) are used as the base for selecting the bathymetric data of other sources. Two other swath bathymetric data sets, the Hydrosweep data of EW9509 cruise and the SeaMARC II swath bathymetric data of MW9006 cruise (Table 1), match well with the ACT bathymetry, thus have been used to extend the base coverage.

For the areas not covered by the swath bathymetry, depth soundings from single-beam echo sounder profiles were used to construct the DEM. R/Vs Ocean Researcher I, Ocean Researcher II, and Ocean Researcher III provide a dense coverage of bathymetric data in the nearshore area of Taiwan, while the underway bathymetric data from the U.S. National Geophysical Data Center (NGDC) provide most bathymetric controls away from Taiwan. Stringent data quality control procedures were applied to single-beam sounding data. Both internal and external crossover error analyses (Smith, 1993) have been performed (Figure 3). The internal crossover error is the difference of depth soundings at the intersection of two tracks from the same cruise, while the external crossover errors indicate the bathymetric difference between different cruises. Ship track data without good self-consistency (*i.e.*, with large internal crossover errors) were rejected. Among the single beam sounding data used in compiling this DEM, except for the NGDC data set which contains sounding data from old cruises, over 95% of the data from Ocean Researcher I, II, and III have their internal crossover errors less

Table 1. DEM Data Sources

Data Type	Data Description	Year Data Collected	Data Points
Swath	ACT (Dual EM12, decimated)	1996	1,944,521
Bathymetry	EW9509 (Hydrosweep)	1995	10,995,765
	MW9006 (SeaMARC II)	1990	135,504
Single Beam	OR I: Various Cruises	1989-1997	256,127
Sounding Data	OR II: Cruise no. 8-264	1992-1997	525,206
	OR III: Cruise no. 70-360	1994-1997	325,931
	NGDC: Various Cruises	1969-1990	235,106
Digitized Data	Digitized from bathymetry and navigation charts		48,099
ETOPOS	Global digital database of land and sea floor elevations on a 5 arc-minute grid.		
GTOPO30	Global digital elevation model on a 30 arc-second grid for land area.		
MEST	Global digital seafloor topography data on 2 arc-minute grid obtained from shipboard depth soundings combined with estimated depth from gravity data derive from satellite altimetry. Compiled by Smith and Sandwell (1997).		
Total Data Points Compiled (excluding global data sets)			14,466,259

than 5% (Figure 3). The external crossover errors are somewhat larger; still, about 90% of these data have their external crossover errors less than 10%. To avoid contamination of the swath bathymetry, single-beam-sounding values which fall inside the area covered by swath bathymetry were not used in the compilation.

In the area south of the Ryukyu Islands, bathymetric data were derived from digitizing the



Fig. 2. Distribution of the bathymetric data used in compiling the new DEM. Gray scale shows spatial resolution of the DEM. Dark gray areas represent coverage of swath bathymetry where spatial resolution reaches 1 km. Ship tracks are shown in black lines. Small dots are locations of either digitized depth values or MEST data points.

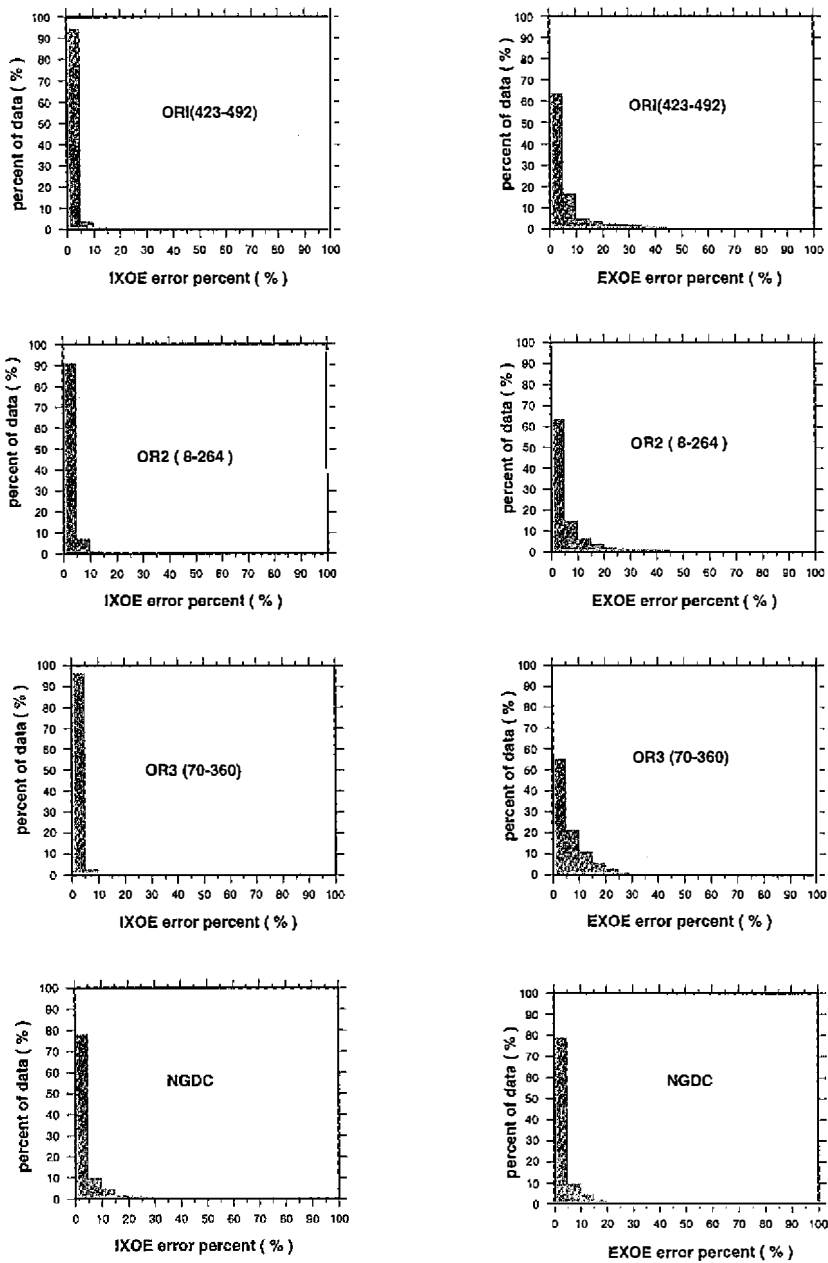


Fig. 3. Internal crossover errors (IXOE) and external crossover errors (EXOE) analyses results of single beam sounding values from R/Vs Ocean Researcher I, Ocean Researcher II, Ocean Researcher III and NGDC data sets. Numbers appeared in the parentheses are cruise numbers of the respective research vessels.

contour lines of the bathymetric map of Hsu *et al.* (1995) which was compiled based on the Seabeam bathymetric maps of Masumoto *et al.* (1993). Near the Penghu Islands and in the western part of the Taiwan Strait, since very few ship track data were available, seafloor depths digitized from navigation charts are used to provide depth controls.

The GTOPO30 data of the study area are used to provide the onland topography. This global digital elevation model provides elevation data at 30 arc-second grid spacing (U.S. Geological Survey, 1993). The MEST data set (Smith and Sandwell, 1997), which provides bathymetric values in 2 arc-minute grid spacing, is used to constrain the seafloor topography wherever large gaps between ship tracks are existed, especially in the Philippine Sea and the South China Sea area. However, large errors were found in MEST for the shallow water region (*e.g.*, the actual water depths in the Taiwan Strait rarely exceed 70 m while the MEST gives depth values over 200 m in many places), and so bathymetric values digitized from navigation charts instead of from MEST data were used to provide basic constraints for the continental shelf region in our DEM compilation.

2.2. Data Processing

Processing and compilation of the bathymetric data involve preliminary processing, editing, gridding, clipping and merging of different source material. Preliminary processing steps include correction and calibration of navigation and sounding data. Preliminary processing of the ACT and EW9509 swath bathymetric data was done onboard the research vessels L'Atalante and M. Ewing, respectively. The SeaMARC II swath bathymetric data were processed at the University of Hawaii. Preliminary processing of all the single beam bathymetric data was performed at the Institute of Oceanography, National Taiwan University. A software package BATHPROC was developed to process and edit different data sets. Gridding and displaying of bathymetric data were performed using the GMT software (Wessel and Smith, 1991).

Editing and compilation of the bathymetric data were based on quality and sounding density of the data sets in a given area. Swath bathymetric data were ranked as the highest quality data, followed by high-density single beam bathymetric data collected by R/Vs Ocean Researcher I, II and III. Single beam bathymetric data from NGDC were ranked third, while the MEST data and bathymetric data digitized from navigation charts used to fill in large gaps between ship tracks were ranked the lowest. Bathymetric data with lower ranks were clipped and excluded from the compilation in areas where data with higher rank were available.

In order to avoid artifacts caused by gridding inadequately sampled data set using a small grid spacing, different gridding intervals were used to evaluate the best grid spacing in a given area. Areas where data density could not support the usage of small grid spacing were clipped and merged with gridded data set of larger grid spacing. Our DEM was generated by merging data sets gridded with 2 arc-minute, 1 arc-minute, 1 km and 500 m spacing, respectively (Figure 2). The data sets with grid spacing larger than 500 m were then interpolated to provide bathymetric values at 500 m spacing. Our final DEM thus contains bathymetric values in 500x500-m grid spacing, thus providing adequate spatial resolution for the area covered by swath bathymetry, while not too large a data set for the whole mapped area.

2.3. Bathymetric Accuracy and Spatial Resolution

The absolute bathymetric accuracy of the DEM varies by areas depending on the data sources. In general, the areas covered by the ACT and EW9509 swath bathymetry have the highest degree of seafloor depth accuracy (less than 1% error). The SeaMARC II bathymetric data have an accuracy of about 3% error margin. External crossover error analyses of densely distributed high quality single beam bathymetric data suggest that 95% of the crossover errors are less than 20 m. External crossover errors for the NGDC data are larger, with about 10% of the data showing crossover errors larger than 40 m. However, only a few of the crossover errors are greater than 60 m. In the area where bathymetric constraints are provided mainly by the MEST data, bathymetric accuracy is the poorest. Hwang (1997) suggested that the RMS error in bathymetric values estimated from Satellite gravity data is about 8%.

Even though the DEM provides depth values in 500x500-m grid spacing, a spatial resolution of 1 km is achieved only in the areas surveyed by swath bathymetric mapping and extremely dense ship tracks (blackened and dark gray area in Figure 2), where the original bathymetric data have horizontal resolutions better than 300 m. Spatial resolutions of 2 km are achieved for onland topography (using GTOPO30 data) and along closely spaced ship tracks (gray area in Figure 2). 2 arc-minute (about 3.7 km) spatial resolution exists only along survey tracks and around bathymetric control points. Since the poorest bathymetric control points are from 2 arc-minute gridded MEST data set, the poorest spatial resolution of the DEM thus is 4 arc-minutes. In general, this DEM provides bathymetric spatial resolution better than 8 km for the whole mapped area, while spatial resolution of 1 km is achieved in the area off northeastern, eastern and southern Taiwan (Figure 2).

3. GENERAL MORPHOLOGY AND TECTONIC PROVINCES

Figure 4 presents a bathymetric map generated from the DEM while 3-D oblique projections of the region's topography are shown in Figure 5. In general, the continental shelf and slope of the passive Chinese continental margin lie to the north and west of Taiwan. East of Taiwan, the sea floor is characterized by a series of E-W trending topographic features, which include the Okinawa Trough, the Ryukyu Arc, the Hopping, Nanao and East Nanao basins, the Yaeyama Ridge, and the Ryukyu Trench. South of the Ryukyu Trench lies the deep sea floor of the West Philippine Basin. In the westernmost corner of the Philippine Sea, the N-S trending Gagua Ridge along 123°E separates a small basin, the Huatung Basin, from the West Philippine Basin. Off southern Taiwan, N-S trending ridges and troughs are the major morphological features. From east to west, these are the Luzon Arc, North Luzon Trough, Hengchun Ridge and Manila Trench. West of the Manila Trench lies the South China Sea Basin. Besides these major submarine topographic features, there are numerous secondary morphological features revealed on the bathymetric map, such as submarine canyons along the northern slope of the Okinawa Trough and off eastern, southeastern and southwestern Taiwan, small ridges and troughs off southeastern Taiwan, platforms and depressions in the Taiwan Strait, deep sea channels and submarine volcanoes in the Okinawa Trough, etc.

Most of the submarine topographic features around Taiwan are related to regional tectonics, and have been described in various previous studies (*e.g.*, Bowin *et al.*, 1978; Chen, 1989;

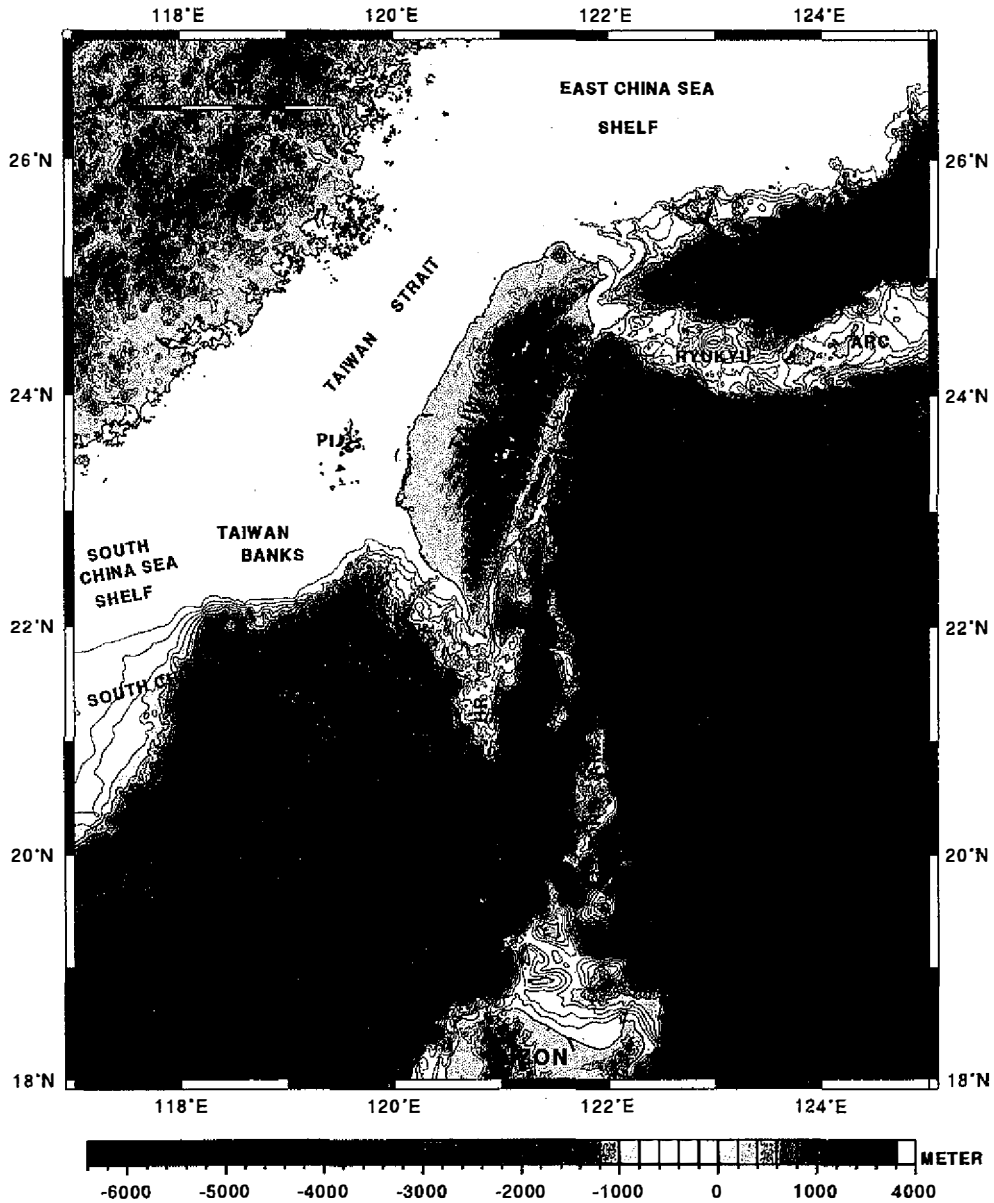


Fig. 4. The DEM bathymetric map offshore Taiwan and its adjacent area. Depth contours in 200-m interval. Elevation contours onland are in 400-m interval. CR: Coastal Range. ENB: East Nanao Basin. FC: Formosa Canyon. HB: Hoping Basin. HC: Hualien Canyon. KC: Kaoping Canyon. PC: Penghu Canyon. HR: Hengchun Ridge. LV: Longitudinal Valley. NB: Nanao Basin. NLT: North Luzon Trough. PI: Penghu Island Group. TC: Taitung Canyon.

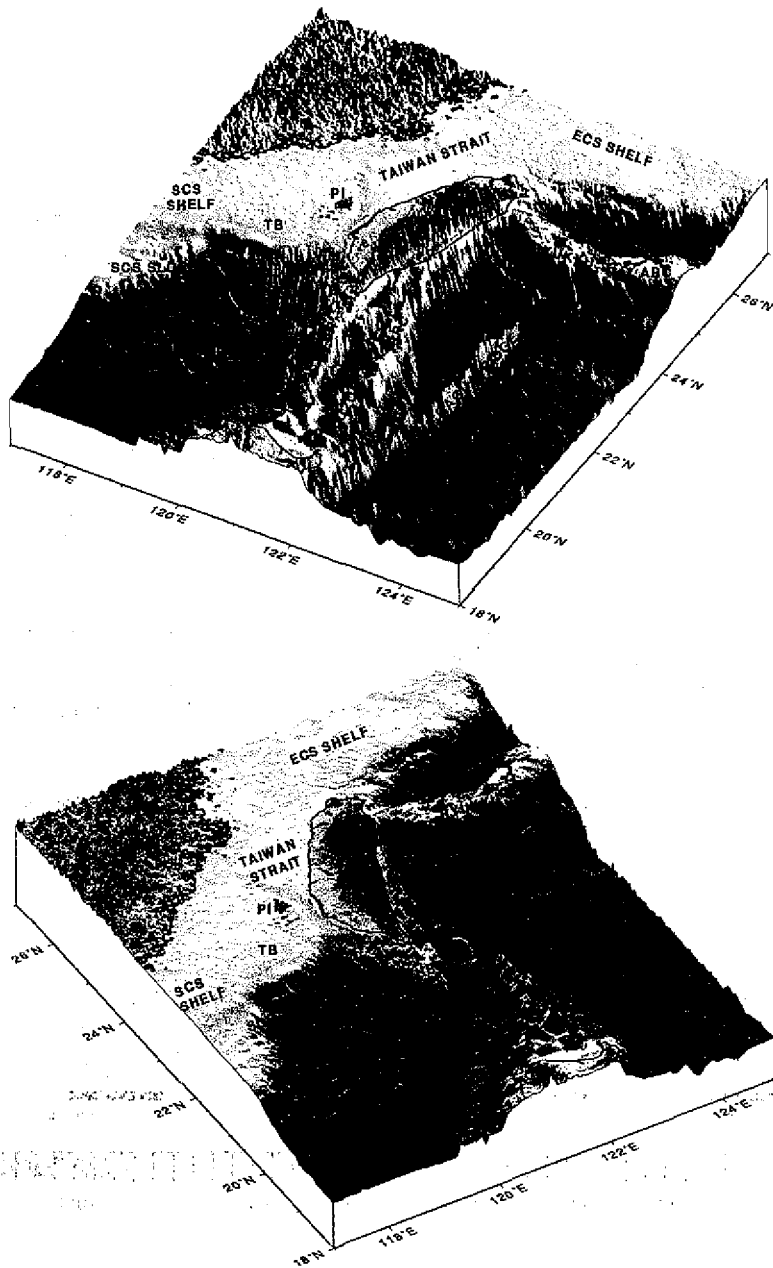


Fig. 5. 3-D physiographic diagrams of Taiwan and its surrounding area. Upper and lower diagrams are generated from two different viewing angles. CR: Coastal Range. ECS: East China Sea. FC: Formosa Canyon. HB: Huatung Basin. HR: Hengchun Ridge. LV: Longitudinal Valley. NB: Nanao Basin. NLT: North Luzon Trough. PC: Penghu Canyon. PI: Penghu Island Group. SCS: South China Sea. TB: Taiwan Banks.

Huang and Yin, 1990; Liu *et al.*, 1992; Huang *et al.*, 1992; Yu and Song, 1993; Liu *et al.*, 1993; Yu and Chiao, 1994; Hsu *et al.*, 1996; Song *et al.*, 1997; Yu, 1997; Sibuet *et al.*, in press). In this study, we divide the areas offshore Taiwan into four tectonic provinces based on their tectonic settings: the passive Chinese continental margin and South China Sea Basin, the Luzon subduction-collision system, the subducting Philippine Sea basins, and the Ryukyu subduction-back arc extension system. In the following sections, we examine in detail the morphological features in each tectonic province as revealed by the DEM and discuss their tectonic implications.

4. CHINESE CONTINENTAL MARGIN AND SOUTH CHINA SEA BASIN

This tectonic province consists of East China Sea shelf, Taiwan Strait, South China Sea shelf and slope, and northeastern part of the South China Sea Basin (Figure 4). The East China Sea slope is presently the northern wall of the Okinawa Trough, and tectonically it is closely associated with the opening of the Okinawa Trough. We consider it to be part of the Ryukyu subduction-back arc extension system, and thus will discuss it in a later session.

Situated along the passive margin of the Eurasia plate, the East China Sea shelf, the Taiwan Strait and the South China Sea shelf and slope are bordered by the Okinawa Trough, the Taiwan mountain belt, and the South China Sea, respectively. Structures of the shelf region are characterized by series of NE-SW trending Tertiary basins in the form of grabens and half-grabens which are bounded by normal faults and covered by Quaternary shelf sediments (Wagemen *et al.*, 1970; Sun, 1982; 1985; Ru, 1988; Sibuet and Hsu, 1997). Sea floor morphology of the shelf region is generally controlled by NE-SW trending extensional structures, and modified by late Cenozoic basaltic volcanism (Chung, 1994) and subaerial erosion during late Pleistocene lower sea level stand (Boggs *et al.*, 1979; Mao and Hsieh, 1989). Topographic features of this province are described below:

4.1 East China Sea Shelf and Taiwan Strait

The East China Sea shelf is a broad shallow surface with small-relief troughs and ridges (Wagemen *et al.*, 1970). The water depth for most of the shelf region is less than 150 m. Due to the lack of adequate bathymetric controls, our DEM can not resolve details of the shelf topography except in the region south of 26°N.

Figure 6 shows a bathymetric map of the southern East China Sea shelf and Taiwan Strait area. Bathymetric contours in general parallel to NE-trending coastline in the southern East China Sea shelf and northern Taiwan Strait. A large bathymetric low, defined by the 60-m contour line, lies in the central part of the northern Taiwan Strait. The depression extends over 300 km from southern East China Sea shelf to the central part of the Taiwan Strait where it terminates north of the Yunchang Rise. The deepest part of this bathymetric low, named the Kuanyin Depression (Chen; 1989), is located near 25°30'N and 121°E, where water depths exceed 100 m (Chen, 1989; Mao and Hsieh, 1989).

Another NE-SW trending bathymetric low, the Wu-Chiu Depression, lies near the coast of China in the western Taiwan Strait. It is about 125 km long and 15 to 18 km wide with an average water depth over 70 m (Mao and Hsieh, 1989). New bathymetric data collected re-

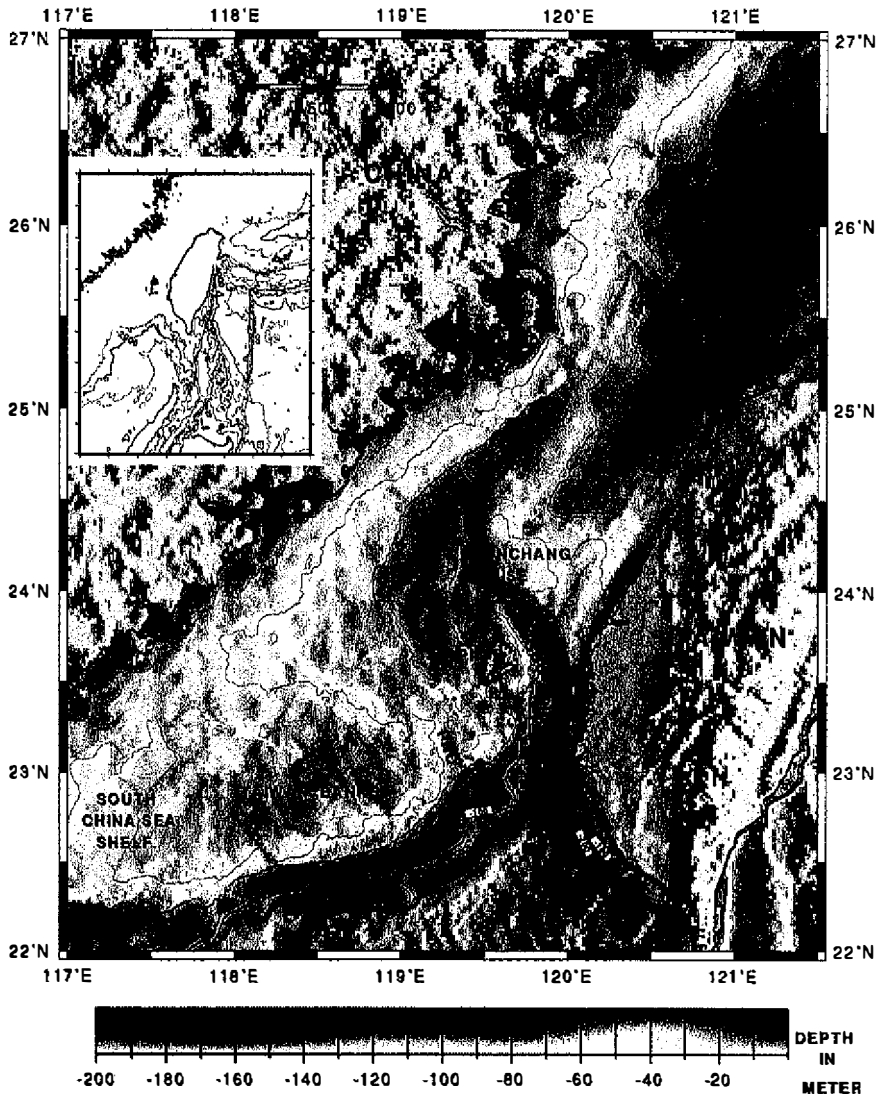


Fig. 6. Shaded bathymetric map of the Taiwan Strait area. Depth contours in 20-m interval except for the 100-m and 200-m contours, which are labeled in the Figure. PI: Penghu Island Group. PNC: Pengnan Channel. WKT: Wangan Kang-Tao.

cently in the central Taiwan Strait reveal that the Penghu channel connects to this depression, and that the southern part of this depression actually extends into the southern Taiwan Strait.

Morphological characteristic of the southern Taiwan Strait is a broad bathymetric low that shallows westward. This bathymetric low is surrounded by the Chinese coast to the west, the Taiwan Banks to the south, the Penghu islands to the east, and the Yunchang Rise to the

northeast. A large submarine channel, the Penghu Channel, lies between the Penghu islands and Taiwan (Figure 6).

The Yunchang Rise is a bathymetric high which extends about 90 km westward from the west coast of Taiwan into the Taiwan Strait (Chen; 1989). Mao and Hsieh (1989), on the other hand, called it the Pengbei (north of Penghu) Rise. This topographic high, expressed roughly by 40-m depth contour line, is probably a relict feature formed during the last glacial period about 15,000 years ago (Boggs *et al.*, 1979; Mao and Hsieh, 1989). Our recent seismic survey data, however, suggest that the southwestern edge of the Yunchang Rise may be controlled by a NNW-SSE trending fault system (Char-Shine Liu, in preparation).

The Penghu island group consists of 64 islands. Most of those islands are covered by Miocene to early Pliocene basalt (Juang and Chen, 1992; Chen and Chang, 1995). Topographically, the Penghu islands can be divided into a northern group and a southern group defined by the 40-m depth contour line (Figure 6). A small NW-SE trending submarine valley separates the northern Penghu island group (consists of Penghu, Paishi, Hsihsu and other small islands) and the southern Penghu island group (consists of Wangan, Chimei, Hua Hsu and other small islands). This submarine valley was called Pa-Chao Kang-Tao (Chinese Navy Chart, 1958) before the island Pa-Chao was renamed to Wangan. It is now called Wangan Kang-Tao (Chinese Navy Chart, 1977).

Taiwan Banks (previously called Formosa Banks) is a large E-W trending bathymetric high lying near the southern end of the Taiwan Strait (Figure 6). It can be defined by the 40-m depth contour line with a large portion of the features shallower than 20 m. There are more than 30 shoals where water depths are less than 15 m in this area (Mao and Hsieh, 1989). The sea floor here is covered by coarse to fine sand and conglomerate. Exposed basement rocks were also found (Mao and Hsieh, 1989). The geological nature of the Taiwan Banks is poorly understood.

A NW-SE trending submarine channel lies along the eastern edge of the Taiwan Banks, separating the banks from the southern Penghu island group. We name this channel the Pengnan (means south of Penghu) Channel. This channel, together with Wangan Kang-Tao and Penghu Channel, provide passages for the southern Taiwan Strait shelf sediments to be transported to the South China Sea Basin.

The Penghu Channel was suggested to be a major branch of the paleo-drainage system on the Taiwan Strait shelf during subaerial exposure approximately 15,000 years ago (Boggs *et al.*, 1979). Our DEM bathymetry confirms that the head of the Penghu Channel connects to the Wu-Chiu Depression near the western edge of the Yunchang Rise. The paths of the Wu-Chiu Depression and the Penghu Channel follow the postulated paleo-drainage system of Boggs *et al.* (1979) well. The Penghu Channel flows southward between Penghu islands and Taiwan, and becomes broader and deeper (over 150 m deep) as it approaches the continental slope. It then joins the Penghu Canyon over the continental slope, as will be described later.

4.2 South China Sea Continental Margin and South China Sea Basin

Our DEM bathymetric data set covers only a small portion of the South China Sea continental shelf west of the Taiwan Banks. The topography of the South China Sea shelf is a low relief shallow surface; however, the South China Sea continental slope shows a distinct varia-

tion from west to east across 118°E. The South China Sea continental slope is a broad gentle slope west of about 117°E. Between 117°E and 118°E, the continental slope narrows from over 210 km to about 50 km in horizontal distance between shelf-slope break and foot of the slope (Figures 1 and 4). Numerous submarine canyons and channels cut across the continental slope south of Taiwan Banks (Figures 4 and 5). Among them, the Penghu Canyon and the Formosa Canyon are two larger ones.

The Penghu Canyon is located along the boundary between the passive South China Sea continental slope and the Kaoping Slope of the Taiwan mountain belt (Yu and Lee, 1993; Liu *et al.*, 1997a). Swath bathymetry mapping in this area reveals that this canyon system was developed by merging a complex system of tributaries, including the Penghu and Pengnan Channels, on the shelf and slope. Details of the Penghu Canyon and the structures controlling its development will be published in a separate paper.

The Formosa Canyon was called the Formosa Bank-South China Sea Submarine Canyon (Figure 4-8 of Yao *et al.*, 1994) and the Tungsha Canyon (Figure 2 of Yao, 1998). However, since the head of this submarine canyon lies near the southwestern end of the Formosa Banks (now called the Taiwan Banks), and it is over 220 km away from the Tungsha Island, we name this canyon the Formosa Canyon. This submarine canyon may be connected to Han Chiang (Han river) of China via submarine valleys across the continental shelf (Figure 5). It extends from the shelf-slope break southeastward over 110 km and joins the Penghu Canyon and the Manila Trench (Figures 4 and 7). The Formosa canyon could be associated with a postulated Manila-Ryukyu transform fault which separates the South China Sea continental margin from the former Ryukyu subduction zone of the Philippine Sea plate (Sibuet and Hsu, 1997). A prominent conical shaped seamount emerges from the seafloor south of the Formosa Canyon at the place the canyon turns eastward (Figure 7). This seamount has a height of over 1000 m above the seafloor and a diameter of about 10 km.

The South China Sea Basin was formed about 32 Ma by the opening of South China Sea (Taylor and Hayes, 1983). Bathymetry of the South China Sea Basin in the mapped area shows that the basin floor in general is deeper than 3600 m and deepens eastward. The Manila Trench forms the eastern boundary of the South China Sea Basin where water depth is over 4000 m.

Taylor and Hayes (1983) put the continent-ocean boundary (COB) along the northern edge of the South China Sea Basin eastward to near 120°E (Figure 1). However, there was little study done previously regarding the nature of the northeastern corner of the South China Sea Basin east of 118°E. Sea floor gravity and magnetic anomaly data compiled recently (Hsu *et al.*, 1998) indicate that the crust in the northeastern corner of the South China Sea Basin is oceanic in nature, and its age should be older than that of the rest of the South China Sea crust. Further investigations are needed to resolve whether this portion of the South China Sea Basin was subsided continental crust, an old piece of the South China Sea crust formed in the early stage of the South China Sea opening, or once part of the Philippine Sea plate as suggested by Sibuet and Hsu (1997).

5. LUZON SUBDUCTION-COLLISION SYSTEM

This tectonic province comprises the area between the Manila Trench and the Luzon volcanic arc off southern Taiwan, and the area off southeastern and off southwestern Taiwan.

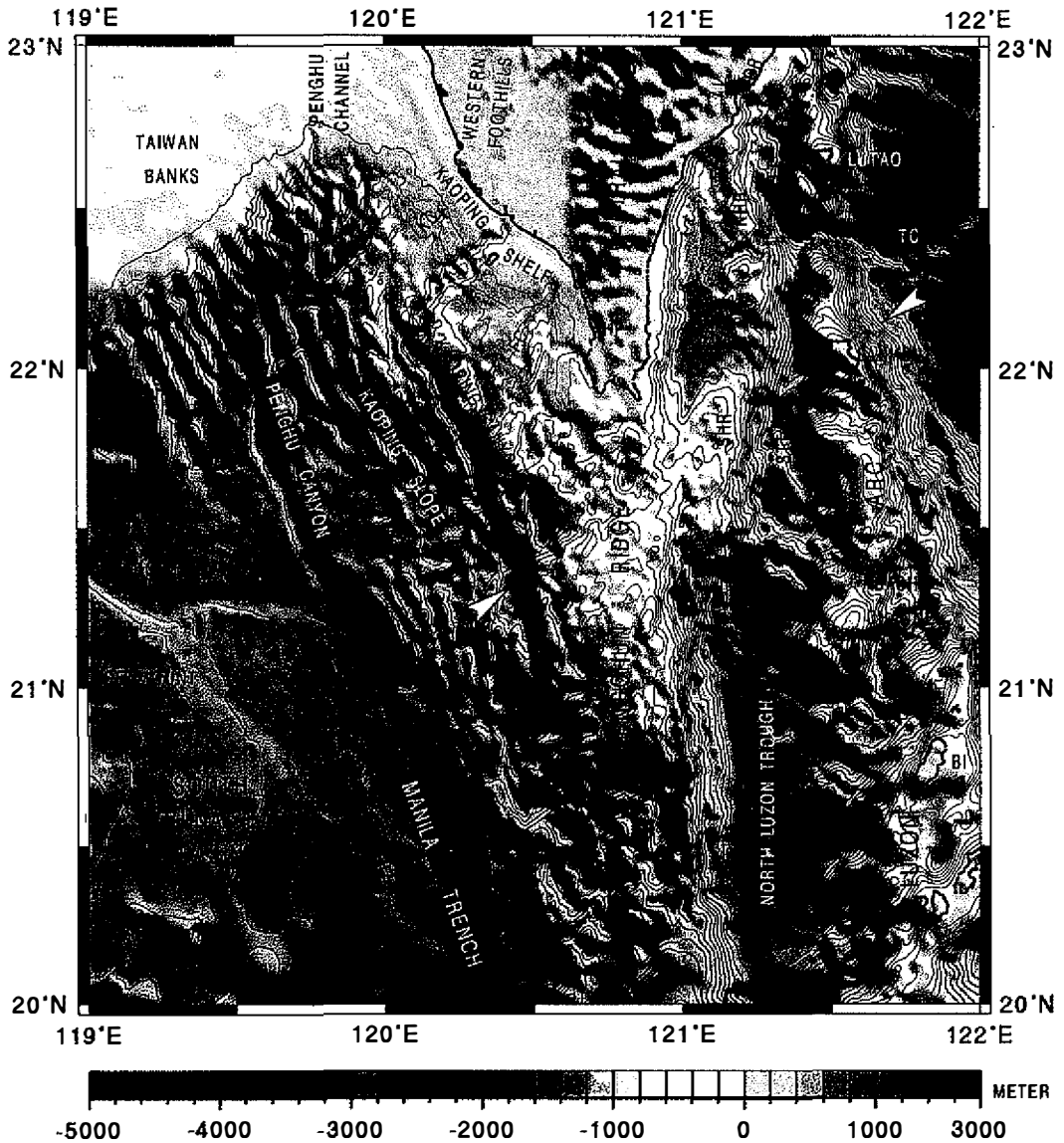


Fig. 7. Shaded bathymetric map off southern Taiwan. Depth contours in 200-m interval. Two arrows indicate the location of a NE-SW trending lineament across the Hengchun and Huatung Ridges, as described in the text. CR: Coastal Range. FC: Fangliao Canyon. HP: Hengchun Peninsula. KC: Kaohsiung Canyon. LV: Longitudinal Valley. NHR: Northern Huatung Ridge. NTT: Northern Taitung Trough. SCS: South China Sea. SHR: Southern Huatung Ridge. STT: Southern Taitung Trough. TC: Taitung Canyon.

This is the area where the Luzon subduction system transforms into the incipient arc-continent collision system (Bowin *et al.*, 1978; Suppe, 1984; Lundberg *et al.*, 1992; 1997; Reed *et al.*, 1992; Huang *et al.*, 1992; Liu *et al.*, 1997). Morphologic features in this province reflect very well with the tectonic activities of the region. Many features have been described in previous publications (*e.g.*, Chen and Juang, 1986; Huang and Yin, 1990; Liu *et al.*, 1992; Reed *et al.*, 1992; Yu and Chiao, 1994; Liu *et al.*, 1997), here we give an overview of the morphologic features of this province as revealed by the new DEM bathymetry (Figure 7).

5.1 Morphology of the Luzon Subduction Zone

In the area south of about 21°N, submarine topography presents the morphology of a typical subduction zone (Figure 7). The western boundary of this subduction zone is the Manila Trench where the South China Sea crust subducts beneath the Philippine Sea plate. Water depth of the trench is deeper than 4200 m west of the Luzon island, and shallows northward. The trench is oriented in a NE-SW direction from 18°N to about 20°N, and then it turns into a NNW-trending direction toward the Chinese Continental margin (Figures 4 and 7). The change in azimuth could simply be the results of outward growth of the accretionary wedge near Taiwan, or it could have resulted from a tectonic event, such as the passage of a transform fault (Sibuet and Hsu, 1997; J.-C. Sibuet, 1998, personal communication). The Manila Trench loses its morphological characteristics as it shallows toward the Chinese continental margin. By definition, the Manila Trench should end where subduction of the South China Sea crust ceases. However, since the changing of tectonic processes from subduction to collision do not happen abruptly, the actual termination location of the Manila Trench is not certain. We extend the Manila Trench northward to about 20°15'N where the Penghu and Formosa canyons join the trench. This is also the latitude where arcward bending of the NNW-SSE trending ridges occur in the frontal portion of the Hengchun Ridge, and the termination of the North Luzon Trough east of the Hengchun Ridge (Figure 7).

The N-S trending Hengchun Ridge is an accretionary wedge. The width of this ridge increases from about 70 km at 20°N to over 110 km near the southern tip of Taiwan (Reed *et al.*, 1992). The depth of the Hengchun Ridge shallows northward, then drops into an ENE-WSW trending topographic low before raising again to connect to the Central Range of Taiwan. The frontal portion of the accretionary wedge shows a gentle dipping lower slope and a slightly steeper upper slope (Reed *et al.*, 1992), while the rear side (arc side) of the accretionary wedge shows a very steep slope toward the forearc basin. The N-S trending steep wall on the rear side of the accretionary wedge is truly remarkable when viewed on shaded 3-D topographic diagrams (Figure 5). This topographic feature extends northward along the western side of the Hengchun Peninsula and connects to the Longitudinal Valley onland Taiwan. This steep wall could be formed by back-thrusts along the rear side of the accretionary (Reed *et al.*, 1992; Lundberg *et al.*, 1997), or due to a normal fault (Byrne, 1995).

East of the Hengchun Ridge lies the North Luzon Trough, a 120-km long and 36-km wide forearc basin. Water depth of this basin is about 3600 m. It is filled with thick (up to 3.5 s twt) orogenic sediments from Taiwan and slump deposits from the accretionary wedge and the volcanic arc (Lundberg *et al.*, 1992). The Luzon volcanic arc forms the eastern boundary of

the North Luzon Trough. This arc lies about 170 km east of the Manila Trench (Figures 4 and 7). Several volcanic islands emerge above the sea level, such as the Batan islands east of the North Luzon Trough and the Lanhsu and Lutaio islands off southeastern Taiwan.

Morphology of the N-S trending Luzon subduction system becomes complex northward where the Luzon Arc collides with the passive Chinese continental margin. The forearc region is being deformed and closed while the frontal portion of the accretionary wedge widens as the influx of orogenic sediments from Taiwan mountain belt increases. The morphology and structures are different in the frontal portion of the incipient collision zone than that in the forearc region, and so we describe them separately below.

5.2 Frontal Portion of the Incipient Collision Zone

The area off southwestern Taiwan is the place where the arc-continent collision zone encroaches the passive continental margin. Distinctive fold-and-thrust structures of the convergent zone and horst-and-graben structures of the passive margin are separated by the deformation front (Figure 1) which extends from the eastern edge of the Manila Trench and Penghu Canyon NNW-ward to the foot of the continental slope, then turns NE-ward across the continental slope and the Kaoping Shelf, and connects to the frontal thrust of the Taiwan mountain belt on land near Tainan city (Liu *et al.*, 1997a). The Kaoping shelf and slope (Yu and Wen, 1992) are frontal portion of the submarine incipient collision zone which are separated from the South China Sea shelf and slope by the Penghu Canyon (Figure 7).

Prominent morphological features in the Kaoping Slope region are the NNW-SSE trending ridges which turn into NNE-SSW direction near the South China Sea slope and then are buried by the Kaoping Shelf sediments. Structurally, these ridges are the northward extension of the ramp anticlines formed by mostly west-vergent thrusts in the frontal portion of the accretionary wedge (Liu *et al.*, 1997a). They connect to the fold-and-thrust belt of the Western Foothills on land Taiwan northward.

Several submarine canyons cut across the Kaoping Shelf in a NE-SW direction (Figure 7), which include, from east to west, the Fengliao Canyon, the Kaoping Canyon, the Kaohsiung Canyon and the Penghu Canyon. Located between the Penghu and Kaoping canyons, the Kaohsiung Canyon is actually a small submarine valley which starts at the shelf-slope break and terminates in the mid-slope region (Yu *et al.*, 1992). The Fengliao Canyon, which is controlled by a shale diapiric ridge (Yu and Lu, 1995), is a tributary of Kaoping Canyon. The Kaoping Canyon is a major submarine canyon in the region which starts from the mouth of the Kaoping Hsi river, running across the Kaoping shelf and slope and joins the Manila Trench at about 120°E and 21°N (Liu *et al.*, 1993). The Penghu Canyon, which was described in Section 4.2, is another major submarine canyon shaped by the tectonic processes of the region.

5.3 Deformation of the Forearc Region

The area off southeastern Taiwan is the place where transition from subduction to arc-continent collision is occurring. Seafloor physiography of the area are characterized by N-S trending ridges and troughs (Figure 7), and were named, from west to east, the Hengchun

Ridge, the Southern Longitudinal Valley, the Huatung Ridge, the Taitung Trough and the Lanhsu Ridge by Chen *et al.* (1988). The Lanhsu Ridge is a section of the Luzon Arc between Bashi Channel and Coastal Range, while the Coastal Range is the onland portion of the Luzon Arc. Huang *et al.* (1992) discussed the tectonic relationships of those ridges and troughs with the geological provinces onland Taiwan. A complete seafloor bathymetric map and a 3-D physiographic diagram of the area was presented by Liu *et al.* (1992) which reveal morphological changes of the forearc region from subduction to arc-continent collision.

More detailed topographic features are presented in the new DEM bathymetric map (Figure 7). Morphological expressions of forearc deformation start at about 21°15'N where eastward widening of the accretionary wedge begins to close the North Luzon Trough (Lundberg *et al.*, 1997), forcing the forearc basin to become a shallower narrow trough, the Taitung Trough, northward. East-vergent back thrusts along arc-side of the accretionary wedge are mainly responsible for the forearc basin closure and uplifting of the Huatung Ridge (Lundberg *et al.*, 1992; 1997; Reed *et al.*, 1992).

The Taitung Trough can be divided into two sections separated by a topographic high located at 22°17'N in the middle of the trough where water depth is about 2300 m. The Taitung Canyon, which connects to Peinan Taihsi river onland near the city of Taitung, flows southward along the central axis of the northern Taitung Trough. This canyon turns eastward just north of the mid-trough topographic high, cutting across the Lanhsu Ridge then flows eastward into the Huatung Basin. The southern Taitung Trough, on the other hand, is a small closed basin with a basin floor at about 2800 m depth. The deepest part of this small basin is a triangular shaped depression located just west of the Lanhsu island. Water depth in the depression is greater than 3100 m. The southern border of this depression is a NE-SW trending steep slope, along which the seafloor raises about 300 m to the main floor of the basin. This NE-SW trending steep slope may be formed by a NE-SW trending strike-slip fault, to be described later in this section.

Morphologically, the Huatung Ridge, interpreted to be uplifted forearc basin strata (Lundberg *et al.*, 1997) and melange (Huang *et al.*, 1992), is separated into two parts by a broad bathymetric low located at about 21°30'N (Figure 7). A small NE-SW trending canyon cuts across the northern part of the ridge and merges into the Taitung Canyon. Northward, the Huatung Ridge connects to the Coastal Range onland. The southern part of the ridge, on the other hand, connects to the Hengchun Ridge along its western border.

The Southern Longitudinal Trough is a trapped small basin located between the Huatung Ridge and the Hengchun Ridge. This basin, interpreted to be a suture basin (Huang *et al.*, 1992; Lundberg *et al.*, 1997), is filled with orogenic sediments from the Central and Coastal Ranges, thus forming a relatively broad and flat basin floor of 800 to 1200 m deep.

Besides the dominant N-S trending topographic features, several NE-SW trending lineaments can be recognized in the bathymetric map (Figure 7). The most prominent one starts from a topographic low on the western flank of the Hengchun Ridge at about 21°30'N and 120°30'E, extends northeastward across the Hengchun and Huatung Ridges, follows the southern border of a bathymetric depression in the southern Taitung Trough, and extends toward the Lanhsu Island. Another one follows the path of the NE-SW trending submarine canyon that running across the Huatung Ridge, and extends eastward across the Lanhsu Ridge following

the path of the Taitung Canyon. These NE-SW trending lineaments are interpreted to be the morphological expressions of NE-SW trending right-lateral strike-slip faults which were developed in this thrust-fault dominant convergent region by bookshelf rotation processes (Fuh *et al.*, 1997).

6. WEST PHILIPPINE SEA BASINS

The southeastern quadrant of the DEM covers the western corner of the Philippine Sea floor (Figure 1). The most prominent morphological feature on the Philippine Sea floor in the mapped area is a N-S trending linear ridge that runs along 123°E extending from the eastern edge of the Luzon Arc near 20°N to the Ryukyu Trench. This ridge, the Gagua Ridge, separates the westernmost corner of the Philippine Sea floor, the Huatung Basin, from the West Philippine Basin. Since the magnetic anomaly lineations show different orientations on either side of the Gagua Ridge (Hilde and Lee, 1994), this ridge is considered to be associated with a fracture zone (Hilde and Lee, 1984; Karp *et al.*, 1997; Deschamps *et al.*, 1997; Hsu *et al.*, 1998).

Morphological characteristics of the sea floor on either side of the Gagua Ridge are also different. The sea floor of the Huatung Basin is covered by thick orogenic sediments derived from the Taiwan mountain belt (Liu *et al.*, 1997b), while numerous seamounts emerge above a thin layer of sea floor sediment in the West Philippine Basin (Figure 8). The Gagua Ridge has dammed orogenic sediments of the Taiwan mountain belt from being transported into the West Philippine Basin, except through a narrow channel in the Ryukyu Trench located around the northern tip of the Gagua Ridge. The sea floor depth west of the Gagua Ridge is thus about 500 to 600 m shallower than that of the abyssal plain to the east of the Gagua Ridge.

Swath bathymetric mapping conducted north of about 22°N in this province reveal detailed sea floor morphology. We discuss the major observations below:

6.1 Huatung Basin

The Huatung Basin (named after the ACT survey) is surrounded by the Gagua Ridge to the east, the Yaeyama Ridge to the north, and the Luzon Arc to the west and south (Figures 4 and 8). We can divide this basin into three zones: the arc slope, the submarine fan, and the deep-sea basin, with submarine canyons cutting across the first two zones.

The arc slope zone, lying along the western boundary of the Huatung Basin, covers the steep eastern slope of the Luzon volcanic arc from 20°N to about 23°30'N. Topography of the sea floor is very rough in this zone, especially for the section abutting the Coastal Range where the arc has been deforming due to arc-continent collision since about 5 Ma. The average slope of this section is about 6 degrees with water depth increasing from sea level down to about 4000 m in a horizontal distance of about 36 km (Figure 8).

The submarine fan zone lies at the foot of the Luzon Arc slope where huge amount of sediments carried by turbidity currents through the submarine canyons has been deposited. This zone covers the northwestern half of the basin. The sea floor dips gently eastward from about 4000 m in depth to over 5500 m near the Ryukyu Trench. Gravity sliding structures are observed above an unconformity on the seismic reflection profiles across this zone (Liu *et al.*,

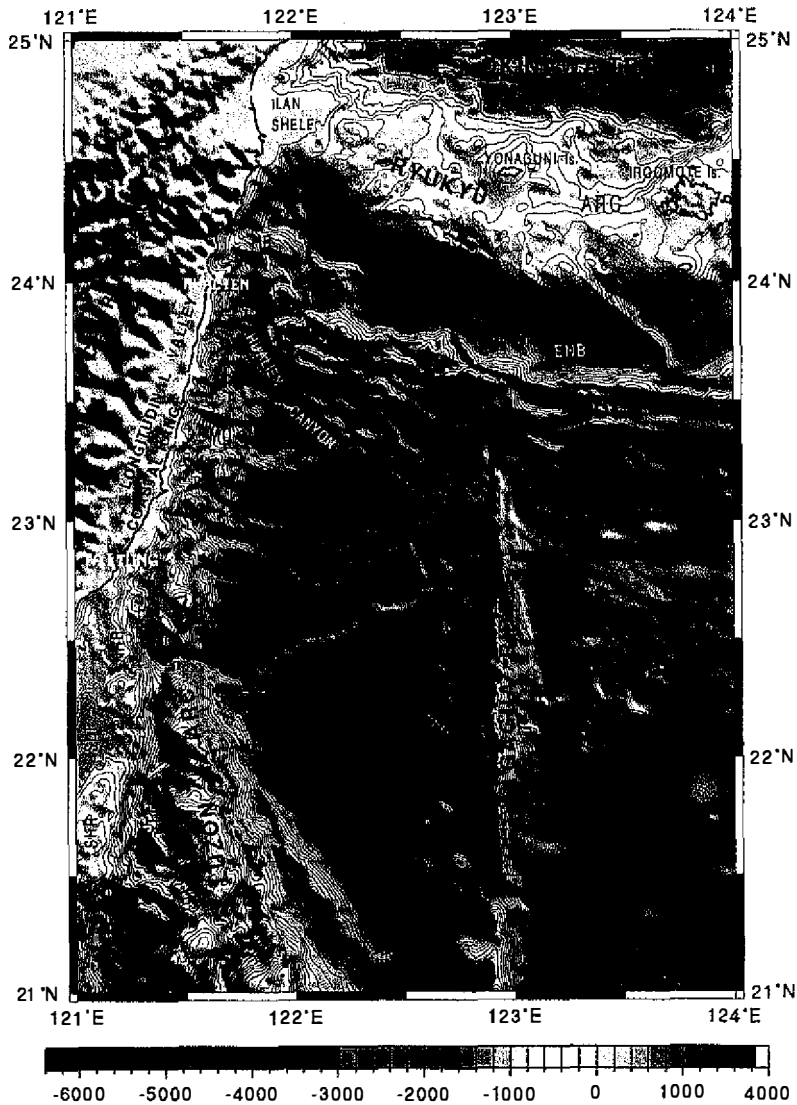


Fig. 8. Shaded bathymetric map off eastern Taiwan. Depth contours in 200-m interval. CMC: Chimei Canyon. ENB: East Nanao Basin. HB: Hopping Basin. HR: Hsincheng Ridge. HRB: Hateruma Basin. NB: Nanao Basin. NHR: Northern Huatung Ridge. NTT: Northern Taitung Trough. SHR: Southern Huatung Ridge. SLT: Southern Longitudinal Valley. STT: Southern Taitung Trough.

1997b).

Numerous submarine canyons cut across the arc slope and submarine fan zones. Most of the canyons are initiated from rivers onland Taiwan. The Hualien Canyon, with its head lo-

cated offshore northern end of the Longitudinal Valley near the city of Hualien, flows eastward around the northern tip of the Coastal Range, then southeastward around the western and southern edge of the Yaeyama Ridge, and finally terminates in the Ryukyu Trench. The overall length of the Hualien Canyon from its head north of the Longitudinal Valley to its tail around the Gagua Ridge at 123°N is about 220 km. This canyon is a morphological boundary between two tectonic units, the Luzon Arc and the Yaeyama Ridge, belonging to the subducting and overriding plates, respectively.

Another major submarine canyon, the Taitung Canyon, originates at southern end of the Coastal Range near the city of Taitung, runs southward in the northern Taitung Trough then eastward across the Luzon Arc between the islands of Luta and Lanhsu, and flows into the Huatung Basin. There, it stretches about 170 km to the northeast where it merges with the Hualien Canyon near the Ryukyu Trench (Figure 8). Detailed morphology and structural controls of this submarine canyon are presented by Schnurle *et al.* (1998b). This canyon serves as a major conduit carrying the sediments from the Coastal Range into the Ryukyu Trench, thus forming a natural boundary separating the submarine fan zone to the northwest and the deep-sea basin zone to the southeast of the canyon.

The volume of sediments carried and the energy of the turbidity currents in some of the submarine canyons are very high. The Chimei Canyon originates from the mouth of the Hsiu-Ku-Luan Hsi river (near 23°30'N and 121°30'E), a large amount of sediment carried in from the Hsiu-Ku-Luan Hsi has blanketed the hills and gullies of the Luzon Arc slope and formed a smooth east-dipping canyon floor which is 8 to 9 km wide (Figure 8). Sediments carried in by the Chimei Canyon have formed a topographic high over the submarine fan at the foot of the slope. Topographic and seismic reflection data reveal that the northern half of this topographic high has been washed away by turbidity currents so that the Chimei Canyon runs directly eastward into the Hualien Canyon (Figure 8). A sharp boundary lies at the foot of the Luzon arc slope between the smooth canyon floor of the upper section and the rough washed-out lower section of the canyon floor. This morphological boundary is interpreted to be the surficial expression of a west-vergent thrust (Lallemand *et al.*, 1997c).

The deep-sea basin zone occupies the southeastern half of the Huatung Basin where the sea floor is very flat. The water depths in the basin range from 4800 to 5000 m. In the eastern part of this zone, a series of small ridges emerge above the flat sea floor. From seismic reflection profiles shown in Bowin *et al.* (1978) and Mrozowski *et al.* (1982), these ridges appear to be connected to the Gagua Ridge underneath a N-S trending trough. The nature of these ridges and their relationships to the Gagua Ridge are not clear yet.

6.2 Gagua Ridge and West Philippine Basin

The Gagua Ridge stands up to 4000 m above the sea floor. The ridge is between 20 to 30 km wide and extends over 350 km along 123°E. Two N-S trending gently sinuous linear crests mark the summit of this ridge, indicating strike-slip deformation (Deschamps *et al.*, 1997). The height of this ridge decreases toward the Ryukyu Trench. Schnurle *et al.* (1998a) suggested that this ridge extends further north and that portion of the ridge has been subducted beneath the Yaeyama Ridge. The indentation of the Gagua Ridge has made a big reentrant in

the deformation front of the Yaeyama Ridge (Figure 8).

The Gagua Ridge was suggested to be an up-faulted sliver of oceanic crust (*e.g.*, Mrozowski *et al.*, 1982; Karp *et al.*, 1997; Deschamps *et al.*, 1997). Deschamps *et al.* (1997) suggested that the axis of the Gagua Ridge corresponds to the trace of a fracture zone. Gravity and magnetic anomaly data, however, reveal a linear basement depression lying just east of the Gagua Ridge and is named the "123E Fracture Zone" (Hsu *et al.*, 1998). Morphologically, this linear basement depression is filled with sediment and appears to be a linear trough with water depths about 5500 m. Further investigations are needed to address the formation of the Gagua Ridge and its relationship to the proposed fracture zone.

The sea floor of the West Philippine Basin presents a rough terrain. The basin floor in general is deeper than 5400 m and deepens toward Ryukyu Trench where water depths exceed 6600 m. The trench floor is filled with sediments derived mostly from the Taiwan mountain belt. Several seamounts pierced through the thick trench fill and stand over 1000 m above the sea floor (*e.g.*, Schnurle *et al.*, 1998a). Due to lack of adequate bathymetric control over a large part of this region, we are unable to provide detailed morphological description here.

7. Ryukyu Subduction-Back Arc Extension System

The Ryukyu subduction-back arc extension system extends from the Kyusyu Island of Japan southwestward to about 127°E, then turns westward and terminates off eastern Taiwan (Figure 1). Convergence between the Eurasia and Philippine Sea plates is oblique to the plate boundary along the southern section of the Ryukyu Trench. The transition from oblique subduction to the arc-continent collision on Taiwan further enhances the complexity of the region.

North of the Ryukyu arc, the Okinawa Trough is expanding owing to back-arc extension processes associated with the subduction of the Philippine Sea plate (Letouzey and Kimura, 1986; Sibuet *et al.*, 1987). The Ryukyu Arc is thus a rifted fragment of continental crust and the present active arc volcanism in the Southern Okinawa Trough is located in the middle of the trough (Sibuet *et al.*, 1987). Even though the subduction and back-arc expansion regimes are related, the morphostructures and mechanisms in each regime are quite different. We examine first the morphology of the subduction complex in the forearc region, then discuss the morphological features in the back-arc region.

7.1 Ryukyu Forearc Region

The morphology of a classic subduction complex is observed in the western portion of the Ryukyu forearc region (Figure 8). Starting at the Ryukyu Trench and moves arcward, the Yaeyama Ridge is a typical accretionary wedge, rising 2000 to 3000 m above the trench floor and trapping sediments between the wedge and arc-slope. Forearc basins in this region have thus formed by the trapping of sediments lying on top of the arc-slope basement (Liu *et al.*, 1997c; Schnurle *et al.*, 1998a).

The Ryukyu Trench can be clearly observed extending westward to about 123°E where the Gagua Ridge enters the trench. West of 123°E, morphological characteristics of the trench are no longer apparent as large amounts of orogenic sediment from the Taiwan mountain belt fill

up the trench floor, leaving only the Hualien Canyon that flows eastward along the toe of the accretionary wedge. The trench may extend all the way to the foot of the Luzon Arc near 122°N, since the subducting Philippine Sea Plate slab extends northwestward under the northern tip of Taiwan (Kao *et al.*, 1998).

The Yaeyama Ridge exhibits a typical accretionary wedge morphology with imbricated folds and thrust ramps distributed across the ridge. A noticeable E-W trending slope break in the frontal portion of the accretionary wedge is observed east of the Gagua Ridge reentrant at 123°E. This slope break is interpreted to be an out-of-sequence thrust formed after the passage of subducted Gagua Ridge (Schnurle *et al.*, 1998a). Then, along the crest of the accretionary wedge in the rear portion of the ridge, a prominent E-W trending linear fracture that curves northwestward into the Nanao Basin can be clearly viewed. Another fracture with similar trending pattern is observed near the western end of the Yaeyama Ridge that extends northwestward to the Hsincheng Ridge (Figure 8). These linear fractures are transcurrent right-lateral strike-slip faults developed to accommodate the strain partitioning caused by the oblique convergence processes (Lallemand *et al.*, 1998). Thus, the frontal accretionary wedge is moving westward relative to the arc. The western end of the Yaeyama Ridge is bounded by the Hualien Canyon. The steep western wall of the ridge suggests that active erosion by the Hualien Canyon is shaping the edge of the accretionary wedge.

A small E-W trending ridge lies at the northwestern end of the Yaeyama Ridge. This ridge, named the Hsincheng Ridge, extends eastward into the forearc basin and partially seals the northwestern corner of the forearc basin into a small sub-basin (Figure 8). The Hsincheng Ridge could be formed due to plowing of the Luzon Arc underneath the Ryukyu forearc region.

Detailed bathymetry reveals that the forearc basin in this region comprises a series of small basins, named from east to west the Hateruma Basin, the East Nanao Basin, the Nanao Basin, and the Hoping Basin. The 3400-m deep Hateruma Basin is connected to a NW-SE trending trough on the Ryukyu arc-slope that was formed due to the ongoing differential motion between the Yonaguni and Hateruma segments of the Ryukyu Arc (Lallemand and Liu, 1998). Located west of the Hateruma Basin, the East Nanao Basin is the deepest among the four, with water depth of the basin floor over 4600 m. A SE-NW trending ridge extending from the Ryukyu arc slope forms the boundary between the Hateruma and East Nanao Basin. With a change of bathymetric values over 1200 m between these two basins, this ridge is likely to be structurally controlled.

The East Nanao Basin and Nanao Basin are separated by a basement high. This basement high might be formed due to the subducted portion of the Gagua Ridge (Liu *et al.*, 1997c; Schnurle *et al.*, 1998a). The Nanao Basin is filled with thick turbidities coming from the Taiwan mountain belt; water depth of the basin floor is about 3600 m. West of the Nanao Basin, the water depth shallows to about 3000 m where the Hoping Basin lies. The shallower depth of the Hoping Basin was caused by sedimentation on top of a deformed basin assemblage, the Suaos Basin strata (Lallemand *et al.*, 1997a), together with the Ryukyu arc basement due to the collision of the Luzon Arc with the Eurasia continental margin just to the west (Liu *et al.*, 1996b; 1997c). Controlled by the ongoing arc-continent collision, the Hoping Basin is orientated in a NNW-SSE direction, lying further north than the other three forearc basins. Hsu *et*

al. (1996) proposed that the southward offsets of the Ryukyu arc slope from west to east were caused by three NW-SE trending strike-slip faults that dissect the southern Ryukyu Arc and back-arc region.

Morphology of the northern Hopping Basin floor is controlled by submarine canyons. Submarine canyons developed along the eastern slope of the Taiwan mountain belt, southern flank of the Ilan Shelf slope, and western flank of the Ryukyu arc slope merge into a single canyon at the eastern tip of the Hsincheng Ridge. This canyon, named the Hopping Canyon, is mainly responsible for carrying the orogenic sediments from Taiwan mountain belt to the forearc basins.

7.2 Southern Okinawa Trough

The Southern Okinawa Trough is a 100-km wide trough that narrows westward and terminates at Ilan Shelf. Water depths reach over 2200 m in the central portion of the trough. Though the general trend of the trough is ENE-WSW, linear topographic lows in the center of the trough show an E-W trending en echelon pattern (Figure 9). These E-W trending linear depressions are the centers of active back-arc extension and bounded by normal faults (Sibuet *et al.*, 1998). Groups of volcanoes emerging above the sea floor can be easily identified. Many of these submarine volcanoes are active, as hydrothermal activities have been observed in the Southern Okinawa Trough (Lee *et al.*, 1998). A large NE-SW trending volcanic chain intersects an E-W trending linear depression at about 123°45'E. Sibuet *et al.* (1998) has suggested that this volcanic group was produced by excessive arc volcanism due to melting of subducted asperities.

7.3 East China Sea Slope

Since detailed description of the trough morphology is given in Sibuet *et al.* (1998), here we focus on the morphology and tectonics of the northern wall of the trough, *i.e.*, the East China Sea slope. The East China Sea slope is bordered by the East China Sea shelf landward. The present shelf-slope break generally lies at depth between 120 and 170 m that extends westward from Sekibi Sho (at 25° 54'N and 124° 34'E) to Menhuahsu, a small island located about 55 km northeast off Taiwan. It then turns southward following the edge of the Chilung Shelf to the northeastern tip of Taiwan (Figure 9). Several small islands lie along the shelf break zone, including the Sekibi Sho, the Diao-Yu-Tai islands (Senkaku Shoto) and three small volcanic islands (Pengchiahsu, Menhuahsu and Huapinghsu) to the north of Taiwan. Teng *et al.* (1992) suggested that the small volcanic islands off northern Taiwan were generated by arc magmatism. Wang *et al.* (1998), on the other hand, suggested that these volcanic islands were probably generated by volcanic extrusion due to post-collisional extension in the northern Taiwan area.

The East China Sea slope, which forms the northern wall of the Okinawa Trough, exhibits complicated topographic features. The continental slope west of 124°E is not a simple slope, but can be divided into an upper slope (interpreted to be a steep fault scarp), a tilted continental block (interpreted to be a subsided piece of continent shelf block), and a lower slope. The amount of subsidence for the tilted continental block decreases westward from over 600 m

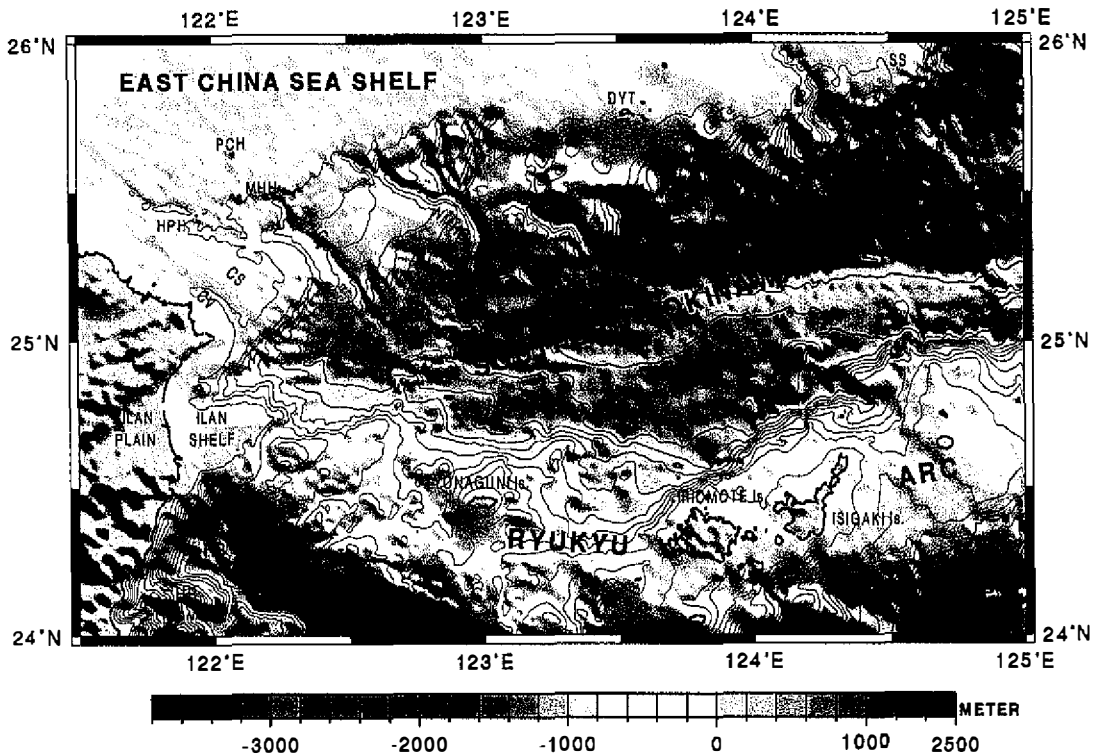


Fig. 9. Shaded bathymetric map of the Southern Okinawa Trough. Depth contours in 200-m interval. CS: Chilung Shelf. CV: Chilung Valley. DYT: Diao-Yu-Tai island. HB: Hoping Basin. HPH: Huapinghsu island. HR: Hsincheng Ridge. MHC: Mien-Hua Canyon. MHH: Menhuahsu island. NMHC: North Mien-Hua Canyon. PCH: Pengchiahsu island. SS: Sekibi Sho.

south of Diao-Yu-Tai Island to almost no subsidence near Huapinghsu (Figures 5 and 9). Song *et al.* (1997) identified two shelf breaks, called the inner shelf break and the outer shelf break, in the region off northern Taiwan. They attributed the deeper outer shelf break to the subsidence of the Chilung Shelf.

A series of submarine canyons have cut across the continental slope and divides the subsided shelf block into several small blocks. The three submarine canyons closest to Taiwan have been named, from west to east, the Chilung Valley, the Mien-Hua Canyon, and the North Mien-Hua Canyon, respectively (Yu, 1992; Song and Chang, 1993). Most of the submarine canyons seem to originate near the shelf-slope break (Figure 9). A few of them may originate from large rivers in mainland China, resulting from subaerial erosion of the present continental shelf during the late Pleistocene lower stand of sea level (Boggs *et al.*, 1979). Boggs *et al.* (1979) suggested that the Mien-Hua Canyon might be connected to the Min River in the Fujian

Province of China (see Figure 5b). The three NW-SE trending submarine canyons north of Taiwan could also be developed along three NW-SE trending strike-slip faults as suggested by Hsu *et al.*, (1996).

Based on the slope morphology revealed from the DEM, we propose that the previous East China Sea shelf extended further south to include the Chilung Shelf and the subsided shelf blocks now lie on the middle of the present East China Sea slope. The present location of the shelf-slope break was developed during the most recent phase of the Southern Okinawa Trough opening which started in late Pleistocene and is still ongoing (Sibuet *et al.*, 1995). This most recent phase of extension probably initiated by post-collisional extension of the Taiwan collision belt. A series of E-W trending normal faults has developed (Sibuet *et al.*, 1998) to accommodate the new N-S trending extension. Part of the previous continental shelf began to subside from east to west, as the opening of the southwestern segment of the Okinawa Trough propagated westward. The present shelf break has developed along an E-W trending normal fault system, which extends from about 124°E to Huapinghsu, leaving a piece of tilted and partially subsided shelf block on the present slope.

8. SUMMARY

Situated in a place where arc-continent collision and flipping of subduction direction are occurring, Taiwan and its adjacent offshore area is a tectonically active region. Morphotectonic characteristics of the seafloor can provide critical constraints on the tectonic processes that produce the submarine topography. A newly compiled DEM covering the offshore region around Taiwan reveals details of the seafloor topography and sheds light on the sedimentary, structural, and tectonic processes of the region.

This DEM was compiled using all the available shipboard bathymetric survey data, supplemented by the global topographic and bathymetric data sets. Stringent crossover error analyses were performed to screen out poor quality sounding data. Proper values for gridding intervals were tested based on the density distribution of the sounding data. In the area where swath bathymetric data are available, a gridding interval of 500 m is selected. In the area where few ship tracks are available, digitized depth values from navigation charts were used to provide bathymetric constraints in the shelf region while the 2 arc-minute gridded MEST data set of Smith and Sandwell (1997) were used to constrain the depth values in the deep sea region. This DEM contains bathymetric data in 500x500-m spacing; however, the spatial resolution of 1 km is achieved only in the area covered by swath bathymetry and densely distributed ship tracks. For most of the areas away from Taiwan, the spatial resolution is 4 arc-minutes.

We have divided the offshore region around Taiwan into four tectonic provinces, namely the passive Chinese continental margin and South China Sea Basin, the Luzon subduction-collision system, the subducting Philippine Sea basins, and the Ryukyu subduction-back arc extension system. Major morphological features in each province as revealed by the DEM are described. Here we summarize the overall morphological characters of the Taiwan offshore region and point out a few interesting observations that may bear significant tectonic implications.

The general morphologic characteristics of the Taiwan offshore area are controlled by the tectonic setting of the region. Continental shelf to the north and west of Taiwan exhibits a low-

relief seafloor that has been modified by subaerial erosion during the last glacial period about 15,000 years ago. Water depths are in general less than 150 m over the shelf region. On the other hand, seafloor of the South China Sea Basin and the West Philippine Basin located to the southwest and to the east of Taiwan, respectively, lie at depth between 3000 m and 6000 m. Two subduction systems extend into Taiwan from east and from south, respectively, and each controls the seafloor topography. Off southern Taiwan, N-S trending ridges and troughs are the dominant topographic features, while east off Taiwan, E-W trending troughs and ridges are pre-dominant.

Submarine canyons are common along the continental slope and the slopes of the Taiwan mountain belt. Some of these submarine canyons are controlled by tectonic structures while others are originated by sedimentary processes.

In the area off southern Taiwan, NE-SW trending lineaments are observed which cut across the dominant N-S trending structures. More prominent E-W to NW-SE trending linear fractures are observed over the Yaeyama Ridge east off Taiwan. These lineaments are probably generated due to the oblique collision and subduction processes.

Four forearc basins were formed along the forearc region of the Ryukyu subduction system. Different seafloor depths of these forearc basins indicate trench-parallel variations of the forearc structures as the tectonic regime changes from subduction to collision.

Back arc extension is active in the Southern Okinawa Trough. Morphology of the East China Sea slope seems to suggest that part of the old shelf has subsided and occupies a portion of the present slope west of 124°E. The amount of subsidence is greater eastward, another indication of the active westward propagation of the Okinawa extension.

Acknowledgments We would like to thank the National Center for Ocean Research for providing the bathymetry data of R/Vs Ocean Researchers I, II, and III. Many of our colleagues, especially H. S. Yu, G. S. Song, C. T. Shyu, M. P. Chen, C. S. Wang and B. Karp have provided the bathymetric data they collected and discussed about the submarine morphological features through various stages of this study. We thank the Captains and crew of the R/Vs Moana Wave, Maurice Ewing, and L'Atalante for their efforts in collecting the swath bathymetry data used in this study. Karen Sender, William Robinson and Andre Le Bot are acknowledged for their efforts in processing the SeaMARC II, Hydrosweep, and EM12 swath bathymetry data, respectively. L. Y. Chao and T. Y. Lee introduced ETOPO5, GTOPO30 and the MEST data sets to us. T. S. Chen and K. C. Wang helped in generating some of the figures used in this paper. Comments made by H. S. Yu, S. K. Hsu, L. Teng, P. Schnurle helped improve this paper. This study presents the results of multi-year efforts in compiling the bathymetric data, which were partially supported by the National Science Council of the Republic of China under grants NSC85-2611-M-002A-003Y and NSC86-2611-M-002A-018-ODP.

REFERENCES

- Boggs, S, W. C. Wang, F. S. Lewis, and J. C. Chen, 1979: Sediment properties and water characteristics of the Taiwan shelf and slope. *Acta Oceanogr. Taiwanica*, **10**, 10-49.
- Bowin, C., R. S. Lu, C. S. Lee, and H. Schouten, 1978: Plate convergence in the Taiwan-

- Luzon region. *Bull. Am. Assoc. Pet. Geol.*, **62**, 1645-1672.
- Byrne, T., 1995: Deformation partitioning and tectonic exhumation in the pre-collision zone of the Taiwan orogenic belt. *EOS, Trans. Am. Geophys. Union*, **76**(46), F635.
- Chase, T. E., and H. W. Menard, 1969: Bathymetric atlas of northwestern Pacific Ocean. U.S. Naval Oceanographic Office H.O. Pub. 1301.
- Chen, M. P., and W. S. Juang, 1986: Seafloor physiography off southeastern Taiwan. *Acta Oceanogr. Taiwanica*, **16**, 1-17.
- Chen, M. P., Y. T. Shieh, and C. S. Shyr, 1988: Seafloor physiography and surface sediments off southeastern Taiwan. *Acta Geologica Taiwanica*, **26**, 333-353.
- Chen, M. P., 1989: Sea floor topography around Taiwan and the plate tectonics. *Science Monthly*, **20**, 579-583 (in Chinese).
- Chen, P. Y., and S. S. Chang, 1995: Geology and Geological History of the Penghu Islands. Penghu County Cultural Center, 239 pp. (in Chinese).
- Chinese Navy Chart, 1958: Peng-Hu Chun-Tao, 1:100,000, Chart No. 331.
- Chinese Navy Chart, 1977: Taiwan Hai-Hsia, 1:650,000, Chart No. 312.
- Chung, S. L., 1994: Late Cenozoic basaltic volcanism around the Taiwan Strait, SE China. *Chem. Geol.*, **112**, 1-20.
- Deschamps, A., S. E. Lallemand, and J. Y. Collot, 1997: The tectonic significance of the Gagau Ridge near Taiwan. International Conference and Sino-American Symposium on Tectonics of East Asia, Programme and Abstracts, 142-143, Chung-Li, Taiwan.
- Fuh, S. C., C. S. Liu, N. Lundberg and D. L. Reed, 1997: Strike-slip faults offshore southern Taiwan: Implications for the oblique arc-continent collision processes. *Tectonophysics*, **274**, 25-40.
- Hilde, T. W. C., and C. S. Lee, 1984: Origin and evolution of the West Philippine Basin: a new interpretation. *Tectonophysics*, **102**, 85-104.
- Ho, C. S., 1986: A synthesis of the geologic evolution of Taiwan. *Tectonophysics*, **125**, 1-16.
- Hsu, S. K., J. C. Sibuet, S. Monti, C. T. Shyu, and C. S. Liu, 1995: Bathymetry map of offshore Taiwan. IFREMER, Brest, France.
- Hsu, S. K., J. C. Sibuet, S. Monti, C. T. Shyu, and C. S. Liu, 1996: Transition between the Okinawa trough backarc extension and the Taiwan collision: new insights on the southernmost Ryukyu subduction zone. *Mar. Geophys. Res.*, **18**, 163-187.
- Hsu, S. K., C. S. Liu, C. T. Shyu, S. Y. Liu, J. C. Sibuet, S. Lallemand, C. Wang, and D. Reed, 1998: New gravity and magnetic anomaly maps in the Taiwan-Luzon region and their preliminary interpretation. *TAO*, **9**, 509-532.
- Huang, C. Y., and Y. C. Yin, 1990: Bathymetric ridges and troughs in the active arc-continent collision region off southeastern Taiwan. *Proc. Geol. Soc. China.*, **33**, 351-372.
- Huang, C. Y., C. T. Shyu, S. B. Liu, T. Q. Lee, and D. D. Sheu, 1992: Marine geology in the arc-continent collision zone off southeastern Taiwan: Implications for Late Neogene evolution of the Coastal Range. *Mar. Geol.*, **107**, 183-212.
- Hwang, C., 1997: Gravity and sea floor topography of South China Sea derived from altimetry data. Proceeding of 1997 Ocean Science Conference, E6-1 ~ E6-8, National Sun Yat-Sen University (in Chinese).

- Jones, T. A., and D. E. Hamilton, 1992: A Philosophy of Contour Mapping with the computer. In: *Computer Methods of Geologic Surface and Volumes*, edited by D. E. Hamilton and T. A. Jones, 1-8, Am. Assoc. Pert. Geol.
- Juang, W. S., and J. C. Chen, 1992: Geochronology and geochemistry of Penghu basalts, Taiwan Strait and their tectonic significance. *Southeast Asian Earth Science*, **7**, 185-193.
- Kao, H., S. J. Shen, and K. F. Ma, 1998: Transition from oblique subduction to collision: Earthquakes in the southernmost Ryukyu arc-Taiwan region. *J. Geophys. Res.*, **103**, 7211-7229.
- Karp, B. Y., R. Kulinich, C. T. Shyu, and C. Wang, 1997: Some features of the arc-continent collision zone in the Ryukyu subduction system, Taiwan Junction area. *Island Arc*, **6**, 303-315.
- Lallemand S. E., C. S. Liu, and Y. Font, 1997a: A tear fault boundary between the Taiwan orogen and the Ryukyu subduction zone. *Tectonophysics*, **274**, 171-190.
- Lallemand, S. E., C. S. Liu, and the ACT cruise scientific team, 1997b: Swath bathymetry reveals active arc-continent collision near Taiwan. *EOS, Trans. Am. Geophys. Union*, **78**, 173-175.
- Lallemand, S. E., S. Dominguez, A. Deschamps, J. Malavieille, and C. S. Liu, 1997c: The southwestern termination of the Ryukyu subduction zone near Taiwan arc-continent collision zone-Results from the ACT cruise. International Conference and Sino-American Symposium on Tectonics of East Asia, Programme and Abstracts, 82-83, Chung-Li, Taiwan.
- Lallemand, S. E., and C. S. Liu, 1998: Geodynamic implications of present-day kinematics in the southern Ryukyus. *J. Geol. Soc. China*, **41**, 551-564.
- Lallemand, S., C. S. Liu, S. Dominguez, P. Schnurle, J. Malavieille, and the ACT scientific crew, 1998: Trench-parallel stretching and folding of forearc basins and lateral migration of the accretionary wedge in the southern Ryukyus: a case of strain partition caused by oblique convergence. *Tectonics*, in press.
- Lee, C. S., G. G. Shor, L. D. Bibee, R. S. Lu, and T. Hilde, 1980: Okinawa Trough: Origin of a back-arc basin. *Mar. Geol.*, **35**, 219-241.
- Lee, C. S., S. L. Chung, and SPOT Members, 1998: Southernmost part of the Okinawa Trough (SPOT): An active extension/collision/subduction area. *EOS, Trans. Am. Geophys. Union*, **79**, W109.
- Lewis, S. D., and D. E. Hayes, 1984: A geophysical study of the Manila Trench, Luzon, Philippines 2. Forearc basin structural and stratigraphic evolution. *J. Geophys. Res.*, **89**, 9196-9214.
- Liu, C. S., S. Y. Liu, B. Y. Kuo, N. Lundberg, and D. L. Reed, 1992: Characteristics of the gravity and magnetic anomalies off southern Taiwan, *Acta Geologica Taiwanica*, **33**, 121-130.
- Liu, C. S., N. Lundberg, D. L. Reed, and Y. L. Huang, 1993: Morphological and seismic characteristics of the Kaoping Submarine Canyon. *Mar. Geo.*, **111**, 93-108.
- Liu, C. S., S. Y. Liu, G. S. Song, C. T. Shyu, H. S. Yu, L. Y. Chiao, C. Wang, and B. Karp, 1996a: Digital bathymetry data offshore Taiwan. 1996 Annual Meeting, Geol. Soc.

- China. Prog-Abstr, 420-425.
- Liu, C. S., S. E. Lallemand, and S. J. Lin, 1996b: Structural characteristics and possible boundary between the Taiwan collision zone and the Ryukyu arc-trench system. Proceedings of Geological Symposium in Memory of Prof. T. P. Yen, 267-275, May 24-25, National Central University, Chung-Li, Taiwan.
- Liu, C. S., I. L. Huang, and L. S. Teng, 1997a: Structural features off southwestern Taiwan. *Mar. Geol.*, **137**, 305-319.
- Liu, C. S., P. Schnurle, S. E. Lallemand, and D. L. Reed, 1997b: Crustal structures of the Philippine Sea plate near Taiwan. International Conference and Sino-American Symposium on Tectonics of East Asia, Programme and Abstracts, 54-55, Chung-Li, Taiwan.
- Liu, C. S., P. Schnurle, S. Lallemand, and D. Reed, 1997c, TAICRUST and deep seismic imaging of western end of the Ryukyu arc-trench system. In Deep Sea Research in Subduction Zone, Spreading Centers and Backarc Basins, edited by K. Fujioka, JAMSTEC Journal of Deep Sea Research, Special Volume, 39-45.
- Lundberg, N., D. L. Reed, C. S. Liu, and J. Lieske Jr., 1992: Structural controls on orogenic sedimentation, submarine Taiwan collision. *Acta Geol. Taiwanica*, **30**, 131-140.
- Lundberg, N., D. L. Reed, C. S. Liu, and J. Lieske Jr., 1997: Forearc-basin closure and arc accretion in the submarine suture zone south of Taiwan. *Tectonophysics*, **274**, 5-24.
- Ma, T. Y. H., 1947: Submarine valleys around the southern part of Taiwan and their geological significance. *Bull. Oceanogr. Inst. Taiwan*, **2**, 1-12.
- Mammerickx, J., R. L. Fisher, F. T. Emmel, and S. M. Smith, 1976: Bathymetry of the East and Southeast Asian Seas: Map and Chart Series MC-17, Geol. Soc. Am. Inc., Boulder.
- Marssett, B., J. C. Sibuet, J. Letouzey, and J. P. Maze, 1987: Bathymetric Map of the Okinawa Trough. Scale 1 : 1,000,000. IFREMER, Brest, France.
- Mao, S. J., and I. H. Hsieh, 1989: Morphology of the Taiwan Strait. In The Investigation and Study on Petroleum Geology and Geophysics in the Western Taiwan Strait, edited by S. P. Nieh, 22-34, Ocean Press, Beijing (in Chinese).
- Matsumoto, T., K. Fujioka, Y. Kato, and M. Aoki, 1993: Detailed bottom topography in the southwesternmost part of the Nanseishoto Trench area. *JAMSTECR*, **30**, 17-36 (in Japanese with English abstract).
- Mrozowski, C. L., S. D. Lewis, and D. E. Hayes, 1982: Complexities in the tectonic evolution of the West Philippine Basin, *Tectonophysics*, **82**, 1-24.
- National Geophysical Data Center, 1988: ETOPO-5 bathymetry/topography data. Data Announcement. 88-MGG-02, National Oceanic and Atmos. Admin., U. S. Dep. Comm.
- Reed, D. L., N. Lundberg, C. S. Liu, and B. Y. Kuo, 1992: Structural relations along the margins of the offshore Taiwan accretionary wedge: implication for accretion and crustal kinematics. *Acta Geologica Taiwanica*, **30**, 105-122.
- Ru, K., 1988: The development of superimposed basins on the northern margin of the South China Sea and its tectonic significance. *Oil Gas Geol.*, **9**, 22-31 (in Chinese with English abstract).
- Schnurle, P., C. S. Liu, D. L. Reed, and S. E. Lallemand, 1998a: Structural insight in the south Ryukyu margin: Effects of the subduction Gagau Ridge. *Tectonophysics*, **288**, 237-

250.

- Schnurle, P., C. S. Liu, D. L. Reed, and S. E. Lallemand, 1998b: Structural insight into the Huatung Basin: Does the Taitung Canyon hide a basement fault? *TAO*, **9**, 453-472.
- Sibuet, J. C., J. Letouzey, F. Barrier, J. Charvet, J. P. Foucher, T. W. C. Hilde, M. Kimura, L. Y. Chiao, B. Marsset, C. Muller, and J. F. Stephan, 1987: Back arc extension in the Okinawa trough. *J. Geophys. Res.*, **92**, 14041-14063.
- Sibuet, J. C., S. K. Hsu, C. T. Shyu, and C. S. Liu, 1995: Structural and kinematic evolution of the Okinawa Trough backarc basin. In: B. Taylor (Editor), *Backarc Basins: Tectonics and Magmatism*. Plenum Press, New York, pp. 343-378.
- Sibuet, J. C., and S. K. Hsu, 1997: Geodynamics of the Taiwan arc-arc collision. *Tectonophysics*, **274**, 221-251.
- Sibuet, J. C., B. Deffontaines, S. K. Hsu, N. Thureau, J. P. Le Formal, C. S. Liu, and the ACT Party, 1998: Okinawa Trough backarc basin: early tectonic and magmatic evolution. *J. Geophys. Res.*, in press.
- Smith, W. H. F., and P. Wessel, 1990: Gridding with continuous curvature splines in tension. *Geophysics*, **55**, 293-305.
- Smith, W. H. F., 1993: On the accuracy of digital bathymetric data. *J. Geophys. Res.*, **98**, 9591-9603.
- Smith, W. H. F., and D. Sandwell, 1997: Measured and estimated seafloor topography. World Data Center-A for Marine Geology and Geophysics Research Publication RP-1, Announcement 97-MGG-03.
- Song, G. S. and Y. C. Chang, 1993: Comment on "Naming of the submarine canyon off northeastern Taiwan: A note" by Ho-Shing Yu (1992). *Acta Ocean. Taiwanica*, **30**, 77-84.
- Song, G. S., 1994: Bathymetry Map Offshore Northeastern Taiwan, Scale 1: 150,000. ROC Naval Hydro. Ocean Office.
- Song, G. S., Y. C. Chang, and C. P. Ma, 1997: Characteristics of submarine topography off northern Taiwan. *TAO*, **8**, 461-480.
- Sun, S. C., 1982: The Tertiary basins of offshore Taiwan. *Proc. Second ASCOPE Conf. and Exhibition*, 1981, Manila, Philippine, 125-135.
- Sun, S. C., 1985: The Cenozoic tectonic evolution of offshore Taiwan. *Energy*, **10**, 421-432.
- Suppe, J., 1984: Kinematics of arc-continent collision, flipping of subduction, and back-arc spreading near Taiwan. *Geol. Soc. China*, **6**, 21-34.
- Taylor, B., and D. E. Hayes, 1983: Origin and history of South China Sea Basin. In D. E. Hayes (Editor). *The Tectonic and Geologic Evolution of Southeast Asian Sea and Island*, 2, Am. Geophys. Union, Washington, DC, 23-56.
- Teng, L. S., C. H. Chen, W. S. Wang, T. K. Liu, W. S. Juang, and J. C. Chen, 1992: Plate kinematic model for the late Cenozoic arc magmatism in northern Taiwan. *Mem. Geol. Soc. China*, **35**, 1-18.
- Teng, L. S., 1990: Geotectonic evolution of the late Cenozoic arc-continent collision in Taiwan. *Tectonophysics*, **183**, 57-76.
- U. S. Geological Survey, 1993: Digital Elevation Models, Data User Guide 5. Reston, Vir-

- ginia.
- Vogt, P. R., and B. E. Tucholke, 1986: Imaging the ocean floor. History and state of the art. The Geology of North Atlantic Region. In: P. R. Vogt, and B. E. Tucholke (Eds.), Geological Society of America, 19-44.
- Wagemen, J. M., T. W. C. Hilde, and K. O. Emery, 1970: Structural framework of East China Sea and Yellow Sea. *Am. Assoc. Pet. Geol. Bull.*, **54**, 1611-1643.
- Wang, K. L., S. L. Chung, R. Shinjo, C. H. Chen, T. F. Yang, and C. H. Chen, 1998: Post-collisional magmatism around northern Taiwan and its relation with opening of the Okinawa Trough. *EOS, Tran. Am. Geophys. Union*, **79**, W109.
- Wessel, P., and W. H. F. Smith, 1991: Free software helps map and display data, *EOS Trans. Am. Geophys. Union*, **72**, 441-456.
- Yabe, H., and R. Tayama, 1928: A cartographical study of the submarine relief of the Strait of Formosa. *Rec. Oceanogr. Works Jpn.*, **1**, 97-101.
- Yao, B., 1998: Crustal structure of the northern margin of the South China Sea and its tectonic significance. *Mar. Geol. Quatern. Geol.*, **18**, 1-16 (in Chinese with English abstract).
- Yao, B., W. Zeng, D. E. Hayes, and S. Spangler, 1994: The Geological Memoir of South China Sea Surveyed Jointly by China and USA. 204 pp., China Geology University Press, Wuhan, China (in Chinese with English abstract).
- Yu, H. S., 1992: Naming of the submarine canyons off northeastern Taiwan: A note. *Acta Oceanogr. Taiwanica*, **29**, 107-112.
- Yu, H. S., C. S. Liu, and J. T. Lee, 1992: The Kaohsiung submarine canyon: A modern aborted canyon and its morphology and echo character. *Acta Oceanographica Taiwanica*, **28**, 19-30.
- Yu, H. S., and E. Hong, 1992: Physiographic characteristics of the continental margin, northeast Taiwan. *TAO*, **3**, 335-370.
- Yu, H. S., and Y. H. Wen, 1992: Physiographic characteristics of the continental margin off southwestern Taiwan. *Jour. Geol. Soc. China*, **35**, 337-351.
- Yu, H. S., and C. T. Lee, 1993: The multi-head Penghu submarine canyon off southwestern Taiwan: Morphology and origin. *Acta Oceanogr. Taiwanica*, **30**, 10-21.10.
- Yu, H. S. and G. S. Song, 1993: Submarine physiography around Taiwan and its relation to tectonic setting. *J. Geol. Soc. China*, **36**, 139-156.
- Yu, H. S., and C. T. Shyu, 1994: Topography, geomagnetism and structure in the self-slope region off northeastern Taiwan. *J. Geol. Soc. China*, **37**, 247-260.
- Yu, H. S., and L. Y. Chiao, 1994: The physiography off southern Taiwan coast: Morphology and its implication for trench-continent convergence. *Acta Oceanogr. Taiwanica*, **33**, 21-37.
- Yu, H. S., and J. C. Lu, 1995: Development of the shale diapir-controlled Fangliao Canyon on the continental slope off southwestern Taiwan. *J. South. Asian Earth Sci.*, **11**, 265-276.
- Yu, H. S., 1997: Characteristics of geological provinces in the offshore area around Taiwan. *Ti-Chih*, **17**, 47-68 (in Chinese).